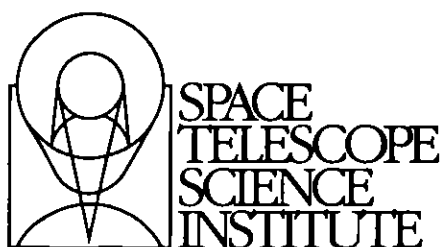

Version 2.0
October 2005

HST Two-Gyro Handbook



Space Telescope Science Institute
3700 San Martin Drive
Baltimore, Maryland 21218
help@stsci.edu

E-mail: help@stsci.edu
Baltimore, Maryland 21218
3700 San Martin Drive
Space Telescope Science Institute
Send comments or corrections to:

(Baltimore: STSCI)
Sembach, K.R., et al. 2005, "HST Two-Gyro Handbook", Version 2.0,
In publications, refer to this document as:

Citation

Version	Date	Editors
1.0	October 2004	Sembach, K.R., et al.
2.0	October 2005	Sembach, K.R., et al.

Revision History

Proposers are strongly encouraged to check the Two-Gyro Science Mode web site throughout the Cycle 15 Phase I proposal period for updates related to two-gyro operations. Other information, not specific to two-gyro operations, can be accessed through the top-level HST web page above.

- URL: http://www.stsci.edu/hst/hts_overview/twogyroMode
- URL: <http://www.stsci.edu/hst> and the HST Two-Gyro Science Mode web site:

Information and other resources are available on the HST web site

World Wide Web

- E-mail: stdesk@eso.org
- The Space Telescope European Coordinating Facility (ST-ECF) also maintains a Help Desk. European users can contact the ST-ECF for help at (800) 544-8125 (U.S., toll free)
- Phone: (410) 338-1082
- E-mail: help@stsci.edu

For prompt answers to any question related to Hubble Space Telescope observations, contact the Space Telescope Science Institute Help Desk at

User Support

Acknowledgments

The information in this Handbook is a brief summary of the experience gained by many individuals working on the HST two-gyro mode development at STScI and elsewhere. Some of the material contained herein is based upon results of the February 2005 two-gyro on-orbit test, as well as documentation and information available at the HST Two-Gyro Phase I Design Review (February 2004) and Critical Design Review (July 2004). Additional material related to guiding performance and pointing jitter is derived from analyses of HST pointing control simulations performed by the HST Pointing and Control Systems group at Lockheed Martin Technical Operations Company. We thank all of the individuals and groups involved in these design reviews and simulations for their efforts. We especially thank Brian Clapp for his efforts in leading the simulation efforts.

The STScI Two-Gyro Team, which assessed the instrument performance results from the February 2005 tests, includes: Santiago Arribas, Ed Bergeron, Carl Biagetti, John Biretta, Colin Cox, Roelof de Jong, Rodger Doxsey, Ron Gilliland, Anton Koekemoer, Vera Kozhurina-Platais, Ray Lucas, Jennifer Mack, Sangeeta Malhotra, Ed Nelan, Keith Noll, Cheryl Pavlovsky, Adam Riess, Kailash Sahu, Glenn Schneider (U. Arizona), Ken Sembach, Marco Sirianni, Tommy Wiklund, and Chun Xu. The STScI Two-Gyro Planning Team for the February 2005 tests includes Allison Vick, George Chapman, and Merle Reinhart.

Ron Downes provided graphical material and helpful text updates for the observation planning portion of this handbook. We thank Susan Rose and Jim Younger for their assistance with the hardcopy and web-based production of the Handbook.

Table of Contents

Acknowledgments	iii
Chapter 1: Introduction to Two Gyro-Mode.....	1
1.1 Introduction	1
1.2 Two-Gyro Pointing and Jitter.....	2
1.3 Scheduling and Target Visibility	3
1.4 Science Instrument Performance.....	5
Chapter 2: Planning Observations in Two-Gyro Mode	7
2.1 Introduction	7
2.2 All-Sky Availability of Fixed Targets	8
2.2.1 Overview.....	8
2.2.2 All-sky Availability Movie.....	9
2.2.3 Number of Available Days During the Course of a Year	9
2.3 Scheduling Considerations and Visibility Periods for Fixed Targets.....	11
2.3.1 Overview.....	11
2.3.2 Unconstrained Fixed-Target Observations.....	12
2.3.3 Constrained Fixed-Target Observations.....	13
2.3.4 Examples	22
2.4 Verifying Scheduling Constraints for Phase I.....	30
2.5 Two-Gyro Orbit Calculations for Phase I.....	30
2.6 Continuous Viewing Zones.....	30
2.7 Moving Targets	31

Chapter 3: The HST Gyroscopes	33
3.1 Gyroscope Overview	33
3.2 Previous Gyroscope Replacements	36
3.3 Overview	37
Chapter 4: Slewinq and Pointing	37
4.1 Overview	37
4.2 Two-Gyro Coordinate Conventions	38
4.3 Pointing Control with Two Gyros	39
4.3.1 Magnetic Sensing System	39
4.3.2 Fixed-Head Star Trackers and Two Gyros (T2G)	40
4.3.3 Fine Guidance Sensors and Two Gyros (F2G)	41
4.3.4 A Typical Sequence of Events for an Acquisition	41
4.3.5 Gyro-only Pointing	43
4.4 Pointing Constraints	43
Chapter 5: Guiding and Jitter	45
5.1 Guiding	45
5.1.1 Guide Star Acquisitions	45
5.1.2 Guide Star Magnitudes	46
5.1.3 Guiding Performance	47
5.2 Jitter Overview	48
5.2.1 Jitter Description	48
5.2.2 Jitter Orientation	48
5.2.3 Sources of Jitter	49
5.2.4 Jitter Frequencies	50
5.3 Disturbances and Primary Sources of Jitter	51
5.3.1 Solar Array (SA3) Disturbances	51
5.3.2 V2 Disturbances	52
5.3.3 High Gain Antenna Motions	54
5.3.4 HTSIM Jitter Simulations	54
5.4.1 Integrated Jitter Predictions	55

Reference Material

Chapter 6: Quiescent F2G-FL Jitter Predictions	59
6.1 HSTSIM Quiescent Jitter Predictions.....	59
Chapter 7: Guide Star Magnitudes.....	61
7.1 Guide Star Magnitude Tables	61
Glossary	65
Index	67

CHAPTER 1:

Introduction to Two Gyro-Mode

In this chapter...

- 1.1 Introduction / 1
- 1.2 Two-Gyro Pointing and Jitter / 2
- 1.3 Scheduling and Target Visibility / 3
- 1.4 Science Instrument Performance / 5

1.1 Introduction



Just interested in the basic two-gyro information needed to submit your Phase I proposal? Read Chapter 1 and Chapter 2. You can skip the reference material found in later chapters.

The Hubble Space Telescope was originally designed to use three rate-sensing gyroscopes to provide fine pointing control of the observatory during science observations. In order to conserve the lifetime of the HST gyros, one of the functioning gyros was turned off on 28 August 2005 and a new attitude control system that functions with only two gyros was activated. In this mode, two gyros used in combination with the Fine Guidance Sensors provide fine-pointing information during science observations.

The *HST Two-Gyro Handbook* contains information about target visibility and scheduling of HST observations conducted with an attitude

The HST Pointing and Control Systems monitored the pointing jitter throughout the two-gyro on-orbit test. For each science exposure, they calculated the jitter at 25 milli-second intervals as estimated by the attitude control law used to maintain the HST pointing. Summaries of the jitter in Table I.I. This table lists the two-gyro peak excursions are given in Table I.I. This table lists the 10-second and 60-second mean, median, and maximum jitter values for the sample of 454 exposures. Almost all of the exposures have a mean jitter less than 10 milli-arcseconds. In a few cases, transient pointing disturbances caused small enhancements in the jitter. These types of disturbances are also commonly seen in three-gyro mode (see Chapter 5 for more information about sources of jitter).



HST fine-pointing performance in two-gyro mode is very similar to the fine-pointing performance observed previously in three-gyro mode.

Gyro #4 will be turned off instead of Gyro #1. The same as the one that will be used in Cycle 15, with the exception that all science observations. The attitude control law used during the test was all science observations. Gyros #2 and #4 were used with the FGS to control the HST attitude during three day tests. Gyro #1 was removed from the pointing control loop, and Specograph (NICMOS), and the Fine Guidance Sensors (FGS) during the Camera for Surveys (ACS), the Near Infrared and Multi-Object Specograph (NICMOS), and the Fine Guidance Sensors (FGS) during the three day tests. More than 450 science exposures were obtained with the Advanced Science instrument performance were carried out on 20-23 February 2005. On-orbit tests of the HST two-gyro fine guiding mode and its impact on science instruments performed out on 20-23 February 2005.

1.2 Two-Gyro Pointing and Jitter

Space Telescope Call for Proposals and Hubble Space Telescope Primer when assembling your Cycle 15 Phase I proposal. The individual Instrument Handbooks contain detailed technical information about the instruments and their on-orbit performance. The Call for Proposals contains policies and instructions for proposing. Use the Handbook on configuration with the appropriate Instrument Handbooks and the Hubble Space Telescope Call for Proposals. Use the Handbook in control system relying upon just two gyroscopes. Use the Handbook

Table 1.1: Jitter Measured During the February 2005 Two-Gyro On-Orbit Test

	Jitter (milli-arcseconds, RMS)			
	Avg 10-sec	Peak 10-sec	Avg 60-sec	Peak 60-sec
Two-Gyro Mean	5.6	6.5	6.0	6.2
Two-Gyro Median	5.5	6.2	5.7	6.0
Two-Gyro Maximum	9.5	22.2	10.7	18.0
Percentage of Two-Gyro Exposures with Jitter < 10 mas	100%	97.8%	99.1%	98.7%
Three-Gyro Mean	4.1	5.2	4.2	4.3

Notes: Two-gyro values are based on a sample of 454 exposures taken during the two-gyro on-orbit test (20-23 February 2005). Three-gyro values are based on a sample of 24 exposures taken several days prior to the two-gyro on-orbit test.

The mean two-gyro 60-second-averaged jitter in Table 1.1 is slightly higher than the mean 10-second-averaged jitter because the sample includes several series of short dithered exposures; the 60-second running averages span short periods of slightly increased jitter between exposures as the pointing was changed from one dither position to the next. The jitter values measured during the two-gyro on-orbit test are only slightly larger than those observed in three-gyro mode. The two-gyro values are similar to those predicted by high fidelity simulations conducted in late 2004 and are comparable to those previously available in three-gyro mode (see Chapter 5 and Chapter 6).

There was no loss of fine lock resulting from large pointing disturbances during any of the science observations obtained in two-gyro mode. Loss of lock occurred for 5 of the 36 acquisitions, but these failures have been traced to either bad guide stars or to a minor problem with roll adjustments during the acquisitions at the beginning of the second orbit of several visits. This latter problem was correctable with a minor change to the flight software. The acquisition success rate in two-gyro mode is expected to be >98%.

1.3 Scheduling and Target Visibility

Observations with either orientation or timing constraints may prove more difficult to implement in two-gyro mode than in three-gyro mode because of the additional pointing restrictions necessary for attitude control

The HST Scheduling Group expects to be able to schedule ~71-73 scheduling efficiency expected for a fully qualified two-gyro proposal pool under two-gyro mode. The results of the study are an approximation to the constraints to make the test proposal pool consistent with implementation designed for three-gyro mode, so it was necessary to change some of the expectations in two-gyro mode. All of the proposals in that cycle were expected in two-gyro mode. Cycle 13 observation pool is a test case to check the scheduling efficiency Cycle had constructed a long range two-gyro scheduling plan using the group had this Handbook was being written, the HST Scheduling

At the time this Handbook was being written, the HST Scheduling

Scheduling Efficiency

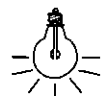
on moving target observations. Chapter 2). See the Cycle 15 Call for Proposals for additional restrictions general scheduling and visibility constraints as fixed targets (see not available in two-gyro mode. Moving targets are subject to the same mode, with the caveats that gyro-only tracking and guide star handoffs are observations in two-gyro mode will work exactly as they did for three-gyro proposers wanting to observe moving targets should assume that

Moving Targets

the Visit Planner in the Astronomers Proposal Tools (APT). the visibility tools available on the Two-Gyro Science Mode web site and Cycle 14. The scheduling information should be used in conjunction with significantly since the initial version of this Handbook was released for two-gyro mode. The information contained therein has not changed consult Chapter 2, which describes the scheduling of observations in observers planning their Cycle 15 Phase I and Phase II proposals should

Fixed Targets

Whenever possible, observers should try to minimize the number of scheduling requirements placed on their observations. This will result in improved schedulability and long range planning, and more efficient use of observing time. Descriptions and examples of how orientation and timing constraints can affect the scheduling of an object and its orbital visibility period can be found in Chapter 2.



in two-gyro mode, compared to >80% of the sky in three-gyro mode. and observatory safety. Roughly half the sky is visible at any point in time

two-gyro prime orbits per week compared to ~80 prime orbits per week in three-gyro mode. Thus, the scheduling efficiency of HST should remain high in two-gyro mode. Cycle 14 long range planning activities will provide additional information about the expected scheduling efficiency for Cycle 15 and future observing cycles.

1.4 Science Instrument Performance

The science instrument performance during the two-gyro on-orbit test was nearly indistinguishable from the science instrument performance in three-gyro mode. Refer to the appropriate Instrument Handbooks for information regarding the detailed on-orbit performance capabilities of the HST science instruments. Additional information about the performance in two-gyro mode can be found in the Instrument Science Reports listed below.

Instrument Science Reports

Characterization of the ACS/HRC PSF in Two-Gyro Mode, (ACS ISR 2005-11), by M. Sirianni et al.

<http://www.stsci.edu/hst/acs/documents/isrs/isr0511.pdf>

Two-Gyro Pointing Stability of HST Measured with ACS, (ACS ISR 2005-07), by A. Koekemoer, V. Kozhurina-Platais, A. Riess, M. Sirianni, J. Biretta, & C. Pavlovsky

<http://www.stsci.edu/hst/acs/documents/isrs/isr0507.pdf>

ACS Coronagraph Performance in Two-Gyro Mode, (ACS ISR 2005-05), by C. Cox & J. Biretta

<http://www.stsci.edu/hst/acs/documents/isrs/isr0505.pdf>

NICMOS Two-Gyro Mode Coronagraphic Performance, (NICMOS ISR 2005-001), by G. Schneider, A.B. Schultz, S. Malhotra, & I. Dashevsky

http://www.stsci.edu/hst/nicmos/documents/isrs/isr_2005_001.pdf

The FGS Astrometry in the Feb. 2005 On-Orbit Two-Gyro Mode Test, (FGS ISR 2005-01), by E. Nelan

http://www.stsci.edu/HST_overview/TwoGyroMode/documents/FGS.pdf

CHAPTER 2:

Planning Observations in Two-Gyro Mode

2.1 Introduction / 7
2.2 All-Sky Availability of Fixed Targets / 8
2.3 Scheduling Considerations and Visibility Periods for Fixed Targets / 11
2.4 Verifying Scheduling Constraints for Phase I / 30
2.5 Two-Gyro Orbit Calculations for Phase I / 30
2.6 Continuous Viewing Zones / 30
2.7 Moving Targets / 31

2.1 Introduction

Observers will face some changes in the way they design their observing programs in Cycle 15 and future cycles. The conversion to two-gyro operations impacts how observations are scheduled and the visibility periods available for scientific observations. This chapter describes the scheduling constraints encountered during two-gyro operations and provides information necessary for observers to successfully complete their Phase I proposal submissions. The material in this chapter has been distilled from a more extensive discussion of the differences between two-gyro and three-gyro operations found in a previous version of this Handbook (v1.0, Ch. 6)

control with either three gyros (top panel) or two gyros (bottom panel). Figure 2.1 shows the sky availability for a single day assuming attitude

Caption: Sky availability for 5 December 2005 in both three-gyro mode (top panel) and two-gyro mode (bottom panel).

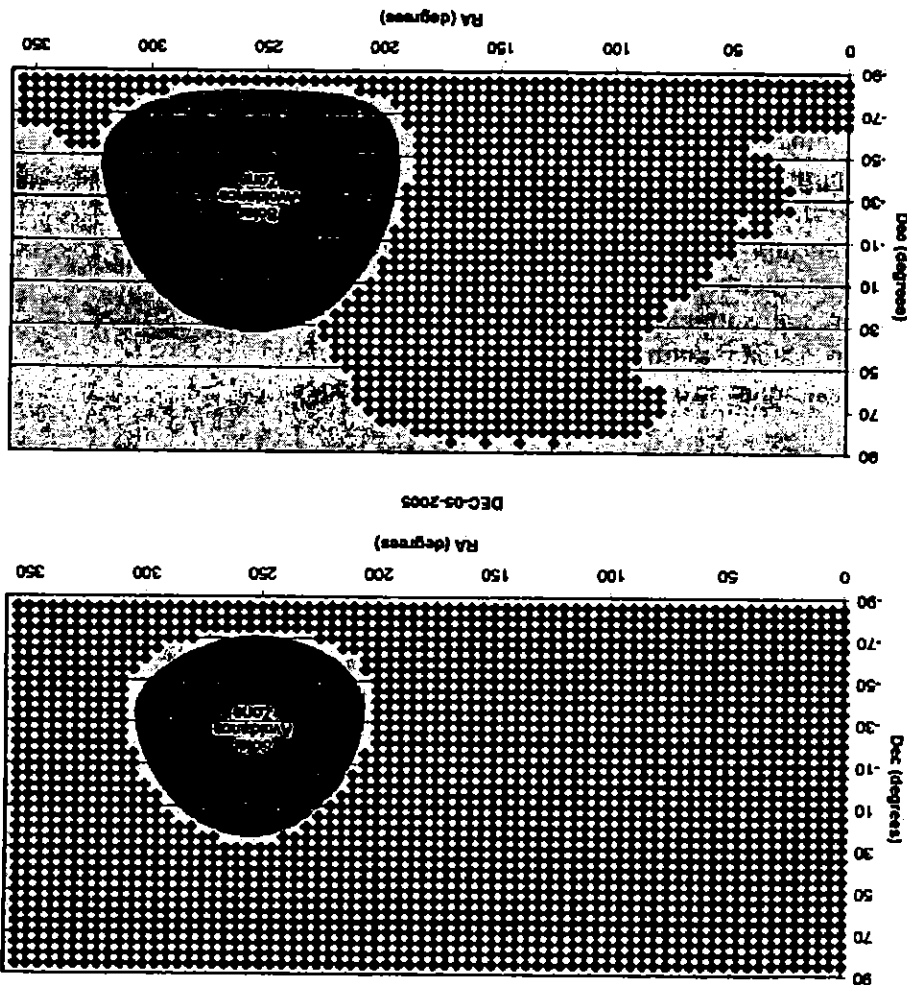


Figure 2.1: Sky Availability on 5 December 2005

The schedulability of an HST observation depends upon many factors and differs considerably between three-gyro and two-gyro operations. To briefly highlight some of these differences, it is useful to compare the accessible regions of the sky in the two modes on a given day of the year.

2.2.1 Overview

2.2 All-Sky Availability of Fixed Targets

Blue regions indicate areas of the sky that can be observed on the date shown, while grey areas of the sky are not observable at that time. The unobservable region of sky is much larger in two-gyro mode than in three-gyro mode because of constraints imposed to achieve guide star acquisitions and to ensure the safety of the observatory. On any given day there is a region of the sky that cannot be observed in either two-gyro or three-gyro mode because of solar avoidance constraints. In three-gyro mode, all regions of the sky outside the solar avoidance zone (50 degree radius) are accessible on any day. The solar avoidance zone for two-gyro mode is larger, with a 60 degree radius. A large region of the sky ahead of the solar avoidance zone (at larger right ascensions than the Sun) is also unobservable in two-gyro mode because of constraints imposed by the process of correcting slew errors and achieving fine guiding lock. Thus, in two-gyro mode most targets can only be observed when they are on the trailing side of the Sun as it moves along the ecliptic. Over the course of the year, all areas of the sky are available in two-gyro mode, but the total time available in any given direction is less than in three-gyro mode.

2.2.2 All-sky Availability Movie

A short narrated movie showing the sky availability during the course of a year can be found on the web at:

http://www.stsci.edu/hst/HST_overview/TwoGyroMode/2GyroMovies/2gyro.html

This movie compares the three-gyro and two-gyro availabilities in one-week increments in a format similar to the figure above. It shows the variable nature of the sky availability in two-gyro mode and the features discussed previously. It also shows that the availability near the equatorial poles is periodic and alternating. This availability pattern at high declinations is tied to the precession of the HST orbit.

2.2.3 Number of Available Days During the Course of a Year

It is useful to consider how many days per year a target of fixed position can be observed by HST. The top panel of Figure 2.2 shows the number of days in a cycle that any position in the sky is observable by HST with three-gyro pointing capabilities. This plot is essentially an encapsulation of the contents of the sky availability movie described above. The color-coding of this figure indicates the number of days for which at least one orbit (defined here to be a contiguous time block of at least 30 minutes) is available to observe a fixed target. In this figure, the allowable Sun angle range is 50-180 degrees. The fewest number of schedulable days occurs over a small swath of sky near the ecliptic, with availability increasing toward the equatorial poles. The minimum number of days available is approximately 260. A large portion of the sky at greater than 50 degrees

The bottom panel of Figure 2.2 shows the number of days in a cycle that any position in the sky is observable with HST in two-gyro mode. Here, the allowable Sun angle range is restricted to 60–180 degrees. Note that the absolute level of the color scaling is different than it is in the three-gyro case shown in the top panel. There are several things worth

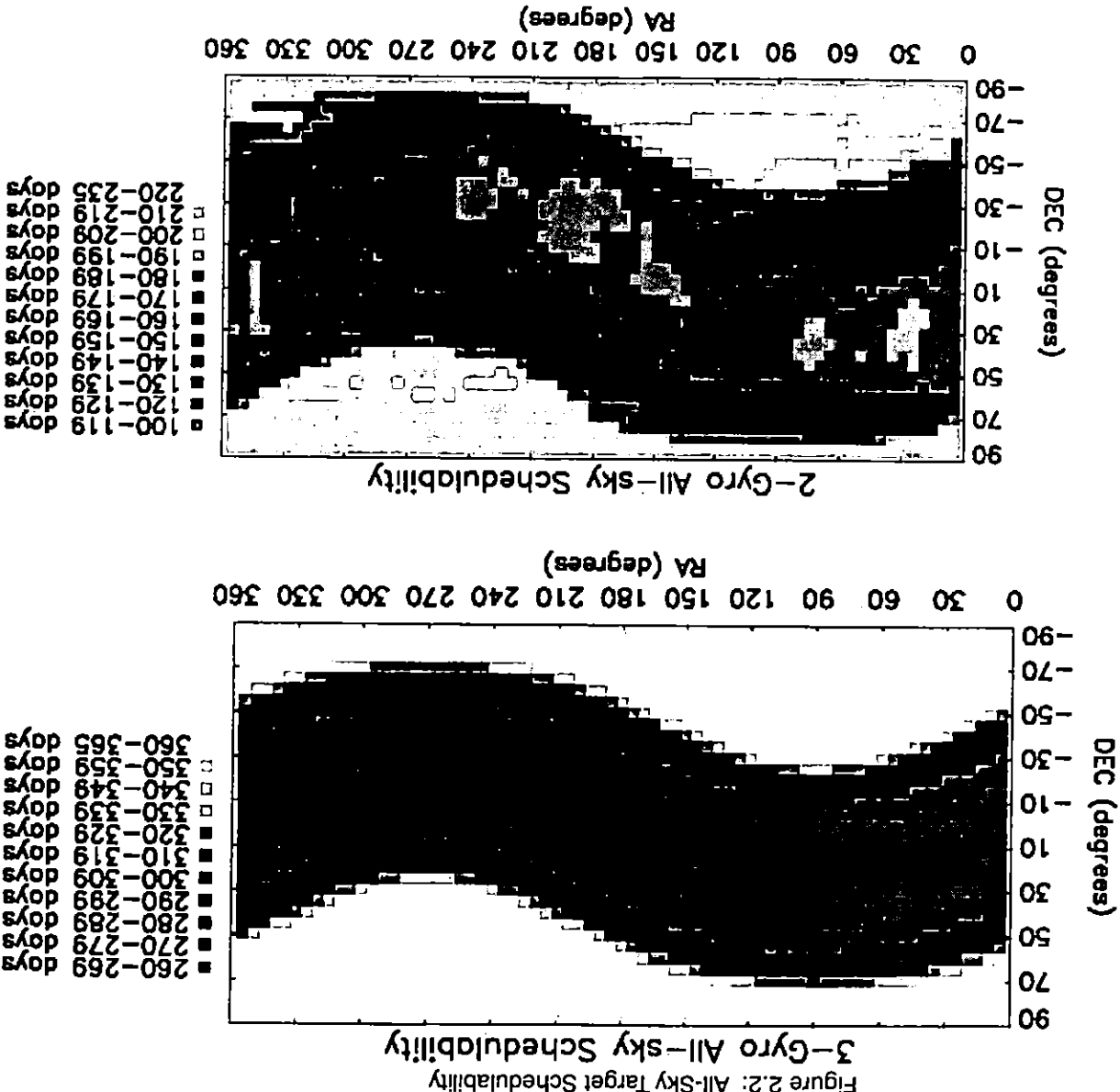


Figure 2.2:

that are described elsewhere (see the *HST Primer* and Section 2.6). CVZ opportunities depend on a variety of additional factors zones (CVZs). Be aware that this plot does not convey the information necessary to judge uninterrupted availability as occurs in the continuous viewing duration. Be aware that this plot does not convey the information necessary ecliptic latitude has at least one schedulable orbit over the entire cycle

noting about this panel when comparing it to the three-gyro results. First, and most importantly, the total number of schedulable days at all positions in the sky decreases substantially in two-gyro mode. Second, the smooth progression in availability seen in the top panel becomes slightly less regular, with pockets of reduced availability occurring across the sky. The overall trend for greater availability increasing toward the equatorial poles remains, but even some high declination pointings have fewer than half as many schedulable days as in three-gyro mode.

2.3 Scheduling Considerations and Visibility Periods for Fixed Targets

2.3.1 Overview

The primary observational constraints on the schedulability of most fixed targets in two-gyro mode are the position of the target in the sky, the required orientation or roll angle of the observatory (if any), and the required timing of the observation (if any). Orientation constraints are usually specified with the ORIENT special requirement and often involve a restricted range of allowable roll angles that correspond to a particular time period that HST is able to achieve this orientation. Timing requirements may be specified either implicitly through the ORIENT special requirement or explicitly through timing special requirements (e.g., BETWEEN, AFTER, etc.). In some cases, an observation may not be schedulable in two-gyro mode because of the restrictions imposed by orientation and/or timing special requirements.



Minimizing the number of special requirements on your observations will improve schedulability.

The operational definition of orbital visibility period for two-gyro operations is the same as it was for three-gyro operations. Orbital visibility is the unocculted time available during the orbit for guide star acquisitions (6 minutes), target acquisitions, science exposures, calibration exposures, and instrument overheads.

Figure 2.3 provides a graphical description of the general decision process involved in determining the schedulability and orbital visibility periods for fixed targets observed in two-gyro mode. The decision process for unconstrained observations involves minimal effort, whereas

If you do not need to specify the orientation of the observatory or the orbital visibility of an unconstrained fixed-target is determined primarily and the observation will be schedulable at some time during the year. The time of year of the observation, then the impact on scheduling is minimized.

2.3.2 Unconstrained Fixed-Target Observations

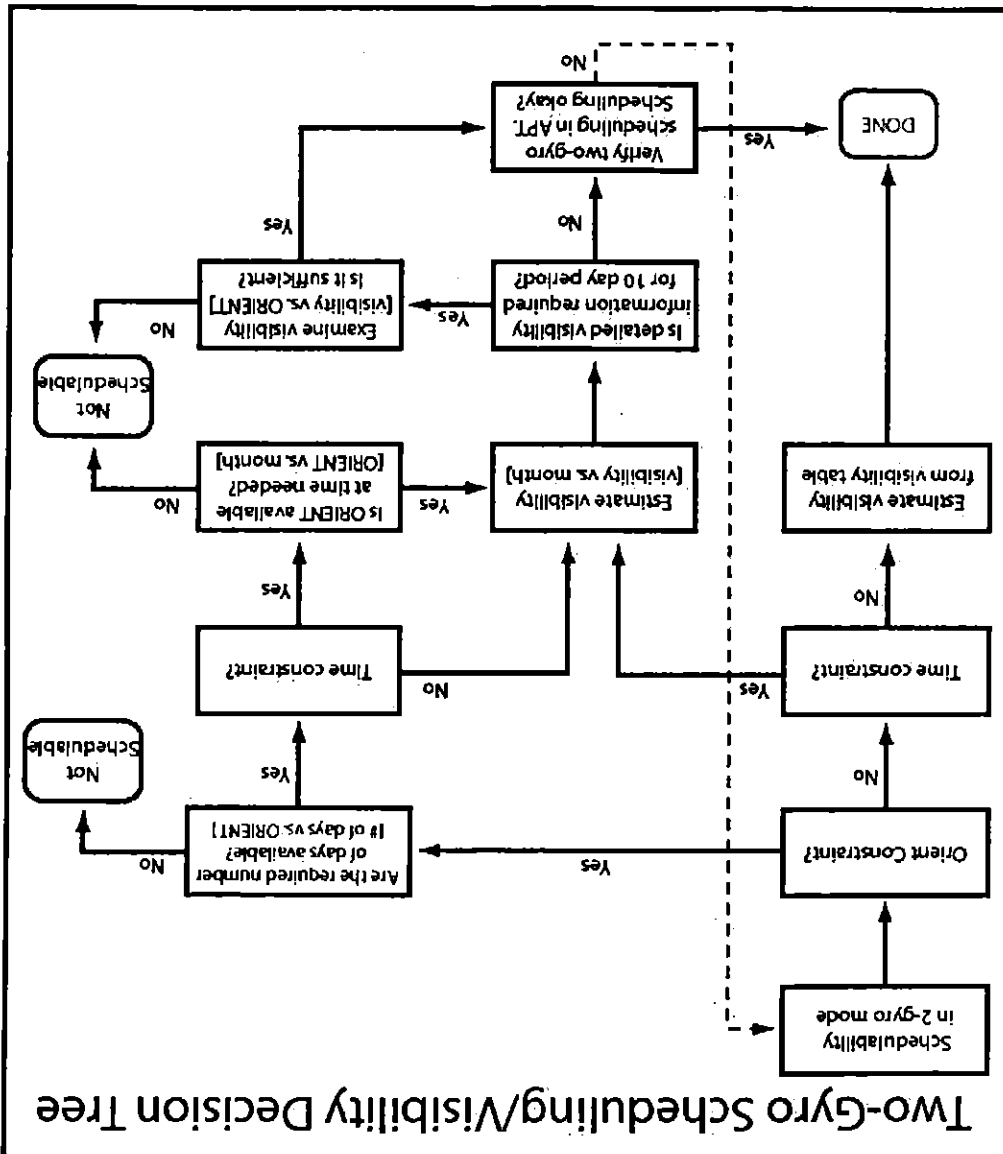


Figure 2.3: Two-Gyro Scheduling and Visibility Decision Tree

constrained observations require more careful consideration of the times of year that an observation can be scheduled. We discuss both types of observations below.

by its declination. Table 2.1 lists the two-gyro orbital visibility periods as a function of declination. These average values are sufficient for Phase I orbit calculations.

Table 2.1: Standard Two-Gyro Fixed-Target Orbital Visibility Periods

Declination (degrees)	Orbital Visibility ¹ (minutes)	LOW Visibility ² (minutes)	SHADOW Visibility ³ (minutes)
0–5	52	47	25
5–15	52	47	25
15–25	53	48	25
25–35	53	48	25
35–45	53	48	25
45–55	54	45	25
55–65	54	45	25
65–75	55	43	25
≥75	57	42	25
Any CVZ	96	incompatible	incompatible

1. The orbital visibility periods in this table are the typical unocculted times available for guide star acquisitions and instrument-related activities.
2. LOW visibility refers to low-sky observations specified with the LOW special requirement.
3. SHADOW visibility refers to Earth-shadow observations specified with the SHADOW special requirement.



If your observation has no timing or orientation special requirements, the orbital visibility period can be found in Table 2.1, and you do not need to use the scheduling plots found later in this chapter or on the Two-Gyro Science Mode web site.

2.3.3 Constrained Fixed-Target Observations

If your science goals require specification of either the orientation of the observatory and/or the timing of the observation, determinations of the schedulability and orbital visibility period are slightly more complicated.

orientations, especially at low declinations, as a result of Sun angle constraints. The range of available orientations expands at higher latitudes, The number of days of availability may be quite limited for some

provided in Table 2.2.

of the table returned by the web tool for the low latitude example is visitabilities ≥ 30 minutes is also plotted in the figures (blue curve). A portion only short visibility periods; for reference, the number of days with listed in Table 2.1 exists (red curve in the figures). Some days may have defined to be one in which at least one orbit with the nominal visibility a high-latitude location ($\alpha = 0^\circ, \delta = +70^\circ$) in Figure 2.5. An available day is orientation for a low-latitude location ($\alpha = 0^\circ, \delta = 0^\circ$) in Figure 2.4 and for achieved in two-gyro mode in Cycle 15 is shown as a function of

The number of days that a particular HST orientation (roll angle) can be

Orientations

Plot Example: Number of Available Days as a Function of

The plots contain information about the schedulability of the target and how much time per orbit is available for the observation. Examples of each of these plots and tables are discussed below.

Cycle 15 and first half of Cycle 16.

3. A plot and table of the target visibility as a function of date during

15 and the first half of Cycle 16.

2. A plot and table of when each orientation is available during Cycle

tation is available.

1. A plot and table of the total number of days per year that each orienta-

web tool include:

The products returned by the Available Science Time and Orientation proposal processing.

Complete models including all constraints will be available for Phase II schedulability of a fixed-target or its orbital visibility significantly. Constraints are not included in these results; this does not alter the constraints expected for two-gyro operations. For clarity, Moon avoidance produce this information rely upon realistic representations of the sky for the Phase I proposal process. The models used as input to provide accurate scheduling and visibility sampling is sufficient to position is within 3.5 degrees of a grid point. This sampling is appropriate for the grid point nearest the input coordinates. Thus, any input were performed on a $5^\circ \times 5^\circ$ grid on the sky. The output returned how long the target is visible. The calculations used to construct this output provides several graphical products that can be used to assess when and for Enter the coordinates of your target into the web form, and the tool provides an on-line tool to help you determine when a fixed target can be scheduled

<http://www.stsci.edu/hst/hsf-overview/twogyromode/allskyinformation>

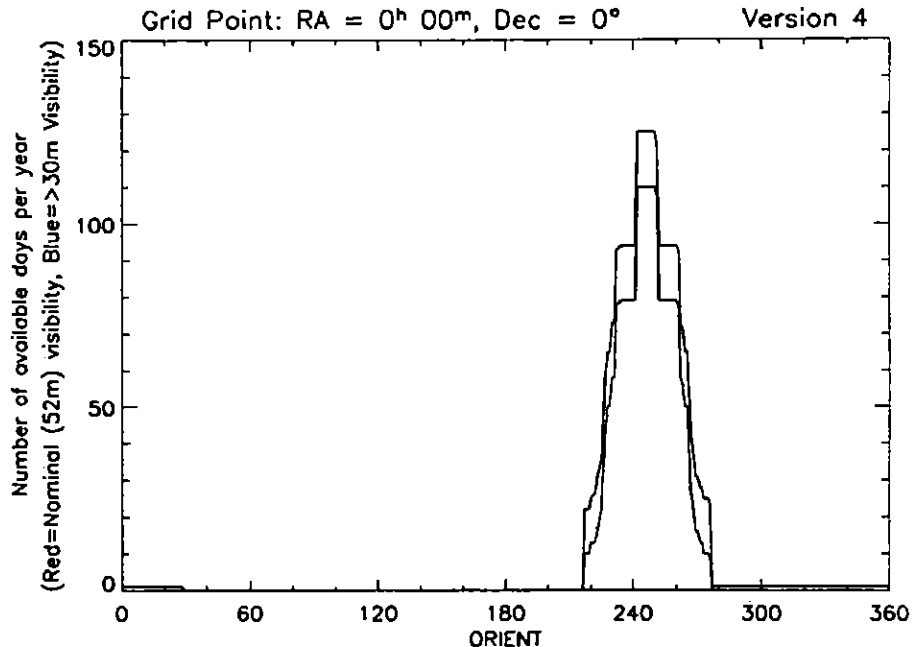
during Cycle 15 is available on the Two-Gyro Science web page at:

An on-line tool to help you determine when a fixed target can be scheduled

with the number of days of availability increasing for some orientations and decreasing for others. In some cases, the number of days available may be zero.

In the low latitude example in Figure 2.4, there is a restricted range of orientations over which the target is observable. There is minimal availability for orientations from 0° - 30° and from 280° - 360° . There is a large window available for orientations centered around 245° , and using orbits with less than the nominal (52 minute) visibility does not increase the availability significantly. Note that, unlike three-gyro operations, it is not possible to observe at orientations with a 180° separation.

Figure 2.4: Orientation Availability for a Low-Latitude Target Near $\alpha = 0^\circ$, $\delta = 0^\circ$



In the high latitude example in Figure 2.5, many orientations are available for five or more days, with notable exceptions occurring over restricted ranges in orientation where the availability dips to zero. Unlike the low latitude case, there are several orientations (e.g., 180°) for which the use of orbits with less than nominal (55 minute) visibility increases the availability; in some cases, the target is available only with these short orbits. However, scheduling these short orbits results in efficient use of the telescope. Requests for short orbits must be well-justified scientifically and are expected to be available only in exceptional cases.

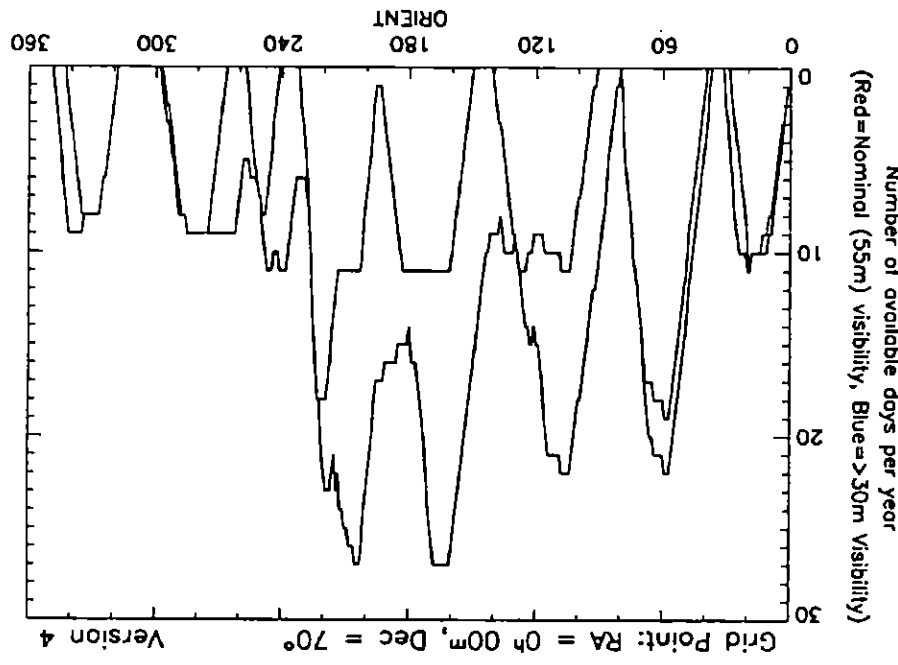


Figure 2.5: Orientation Availability for a High-Latitude Target at $\alpha = 0^\circ$, $\delta = +70^\circ$

Orientations	Number of Days Available (>30 min)	Number of Days Available (>52 min)
:	:	:
272	28	13
271	28	13
270	31	16
269	31	16
268	37	22
267	41	26
266	54	39
265	65	50
264	65	50
263	71	56
262	73	58
:	:	:

Grid Point: RA = 0h 00m, Dec = 0°

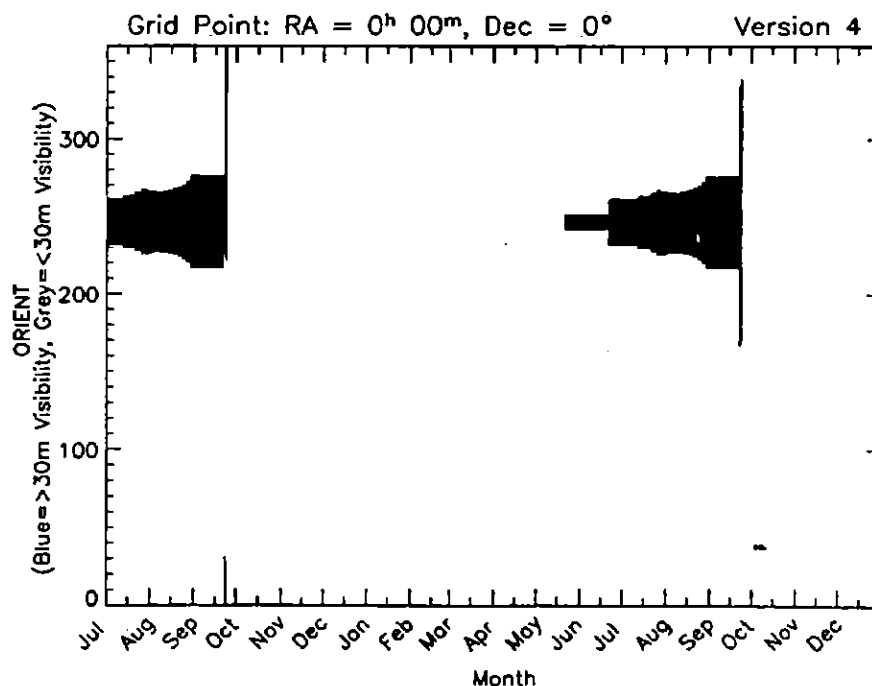
Table 2.2: A Portion of the Tabular Output for the Data Shown in Figure 2.4

Plot Example: Availability of Roll Angles in Cycle 15

If a sufficient number of days exists to observe a target, the next step in determining its schedulability is to check when the target could be scheduled. If there are roll angle (ORIENT) constraints, you should check when the particular orientation is available by examining the web tool plot illustrating ORIENT versus time. Example plots are shown in Figure 2.6 and Figure 2.7, and a sample of the tabular output is shown in Table 2.3. The time axis on these plots extends for 18 months from the start of Cycle 15 (1 July 2006 to 31-Dec-2007) so that observers can judge whether observations that may begin in Cycle 15 could be concluded in the first half of Cycle 16. The blue regions of the figures indicate what orientations are available for the specified date when there is at least one orbit with 30 minutes of visibility. The gold regions indicate less than 30 minutes of visibility for some ORIENTs on that date. Note that most orientations are available only for limited periods of time.

Consider first the low-latitude pointing in Figure 2.6. The February-May time period is unavailable because of Sun avoidance restrictions. The Sun-leading region of the sky (October-February) is also inaccessible in two-gyro mode because of the need for fixed-head star tracker (FHST) visibility prior to fine-lock. Thus, in 2006, available orientations are limited to the June-September timeframe. A somewhat larger range of orientations is accessible for a very restricted range of dates in late September 2006 and 2007 when the target is located near the anti-Sun direction.

Figure 2.6: Low-Latitude Target Roll Angles Available During Cycle 15



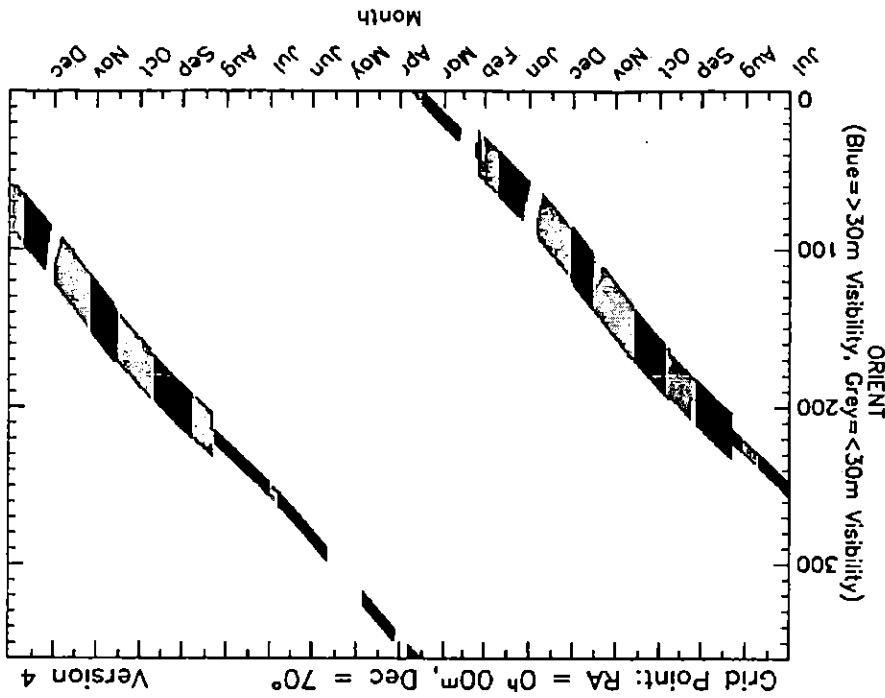


Figure 2.7: High-Latitude Target Roll Angles Available in Cycle 15

Date	Available Orientations
Grid Point: RA = 0h 00m, Dec = 0°	:
20-Sep-2006	216.6 - 276.6
21-Sep-2006	216.6 - 276.
22-Sep-2006	225.6 - 276.6
23-Sep-2006	223.0 - 31.0
24-Sep-2006	221.0 - 28.0
22-May-2007	241.6 - 251.6
23-May-2007	241.6 - 251.6
24-May-2007	241.6 - 251.6
25-May-2007	241.6 - 251.6
Grid Point: RA = 0h 00m, Dec = 70°	Version 4

Table 2.3: A Portion of the Tabular Output for the Data Shown in Figure 2.6

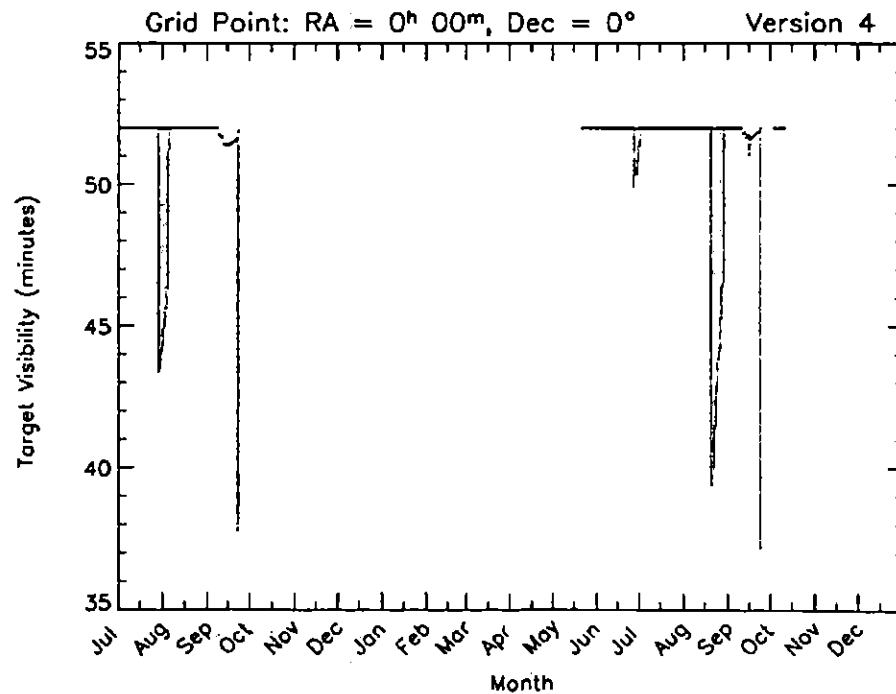
For the high-latitude pointing in Figure 2.7, the availability of roll angles in two-gyro mode is broken into several time intervals separated by periods where the object is unobservable. These breaks in availability occur primarily because precession of the HST orbit causes the Earth to block the FHTSs, which are needed for guide star acquisitions. For the high-latitude pointing in Figure 2.7, the availability of roll angles is broken into several time intervals separated by periods where the object is unobservable. These breaks in availability occur primarily because precession of the HST orbit causes the Earth to block the FHTSs, which are needed for guide star acquisitions.

Plot Example: Target Visibility as a Function of Date

For constrained observations, the orbit visibility may change dramatically throughout the year, unlike unconstrained observations, the visibility cannot be described as a simple function of declination alone (e.g., Table 2.1). The web tool displays the visibility information in graphical form in a plot of target visibility versus time for an 18 month period beginning at the start of Cycle 15 (1 July 2006 to 31-Dec-2007). Plots for the low- and high-latitude sight lines are shown in Figure 2.8 and Figure 2.9. Sample tabular output for Figure 2.8 is shown in Table 2.4. The orbital visibilities in these plots are shown with blue points indicating the maximum visibility available, and by green lines indicating the full range of visibilities for the orientations available. In some instances, the maximum visibility depicted by the blue line may be identical to the minimum visibility in which case there is no green line, just a blue point.

The horizontal black line at 30 minutes in Figure 2.8 and Figure 2.9 indicates the minimum orbital visibility that will be allowed for Phase I proposals in Cycle 15 without special scientific justification. Most observations can be scheduled at times when the orbital visibility exceeds this amount, and those few that cannot will likely have other restrictions that will preclude such observations. For example, in the high-latitude example, the visibility window on 11 September 2006 is only 10 minutes. Therefore, a target at this location in the sky will not be scheduled on this date.

Figure 2.8: Orbital Visibility for a Low-Latitude Target in Cycle 15



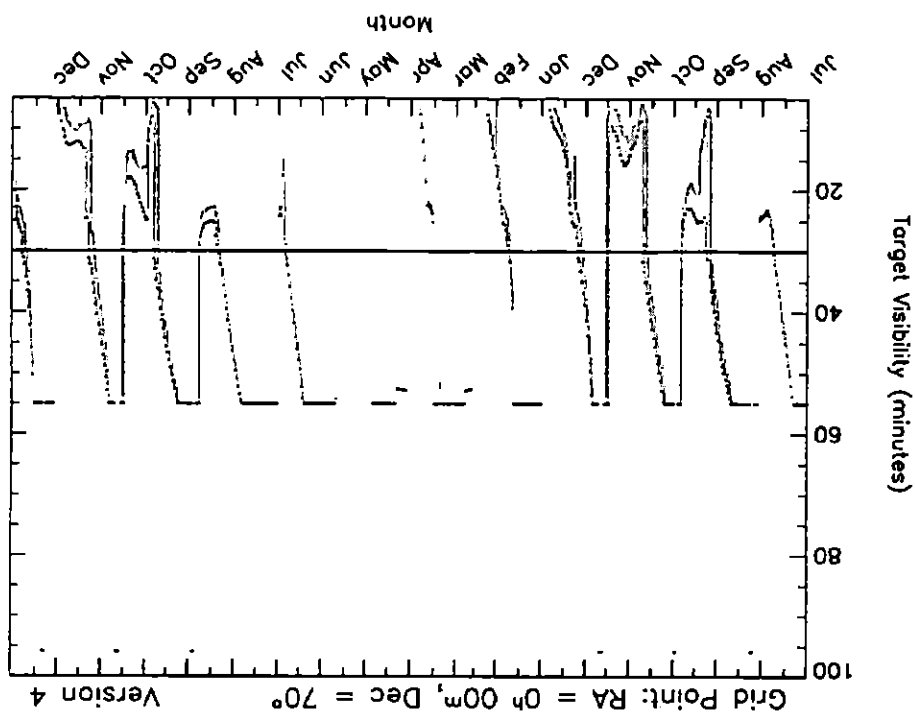


Figure 2.9: Orbital Visibility for a High-Latitude Target in Cycle 15

Date	Science Time Available (minutes)	Two-Gyro (maximum)	Two-Gyro (minimum)
Grid Point: RA = 0 ^h 00 ^m , Dec = 0 ^o	:	:	:
26-Jul-2006	52.0	52.0	52.0
27-Jul-2006	52.0	52.0	52.0
28-Jul-2006	52.0	52.0	52.0
29-Jul-2006	43.3	52.0	52.0
30-Jul-2006	43.4	52.0	52.0
31-Jul-2006	43.6	52.0	52.0
01-Aug-2006	44.0	52.0	52.0
02-Aug-2006	44.3	52.0	52.0
03-Aug-2006	44.9	52.0	52.0
04-Aug-2006	45.5	52.0	52.0
Grid Point: RA = 0 ^h 00 ^m , Dec = 70 ^o	:	:	:
Version 4			

Table 2.4: A Portion of the Tabular Output for the Data Shown in Figure 2.8

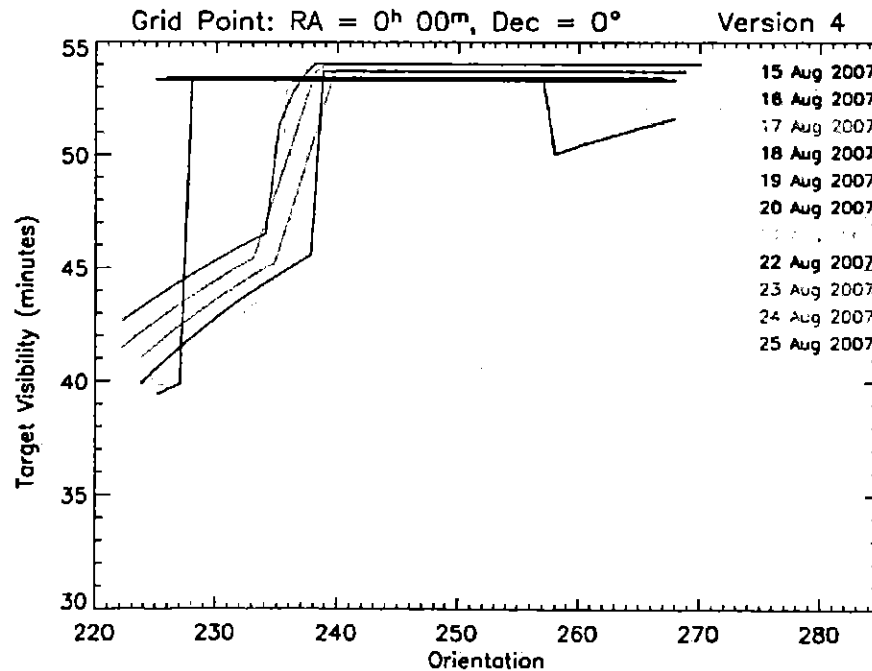
In calculating the orbit visibility period in two-gyro mode for Cycle 15, observers should adopt the maximum visibility estimate indicated by the blue points in the visibility plots unless they have both ORIENT and timing restrictions, in which case they need to examine the more detailed visibility plots described in the next section. The HST scheduling system will make every effort to schedule observations when the visibility is optimized.

Detailed Target Visibility Considerations

In some cases it may be necessary to have a more detailed look at the target visibility for various orientations on a particular date to assess whether a highly constrained observation is feasible. The Detailed Visibility Tool on the Two-Gyro Science Mode web page can be used to determine the target visibility. You can enter the target coordinates and the desired date of the observation, and the tool will return a plot and table of the science time available as a function of orientation for the 11 day interval centered on the input date.

Figure 2.10 contains an example of the detailed visibility plot for the low-latitude sight line example on a set of dates centered on 20 August 2007. The resulting visibilities are color coded by date. The information is shown in tabular form in Table 2.5. Observers requiring a specific orientation on a specific date should specify the appropriate visibility indicated by these plots (or tables) in their Phase I proposals.

Figure 2.10: Detailed Visibility Plot for a Low-Latitude Target



-27°, 55°, respectively. Observer #1 wants to search for supernovae in the HDF and HUDF by repeating a set of ACS observations every ~45 days for as many consecutive 45-day intervals as possible. The fields are tilted with multiple pointings, each of which has five 400 second integrations designed to fit in a single orbit. The total time required to tile either field is 15 orbits (~1 day). Orientation is not critical, as the field can be tilted in a manner that allows nearly full coverage of the field regardless of orientation. The HDF and HUDF are located at $\alpha = 12^{\text{h}} 32^{\text{m}}$, $\delta = +62^{\circ} 18'$, and $\alpha = 3^{\text{h}} 32^{\text{m}}$, $\delta =$

Example 1: Time-series observations of the Hubble Deep Field (HDF) and Hubble Ultra Deep Field (HUDF).

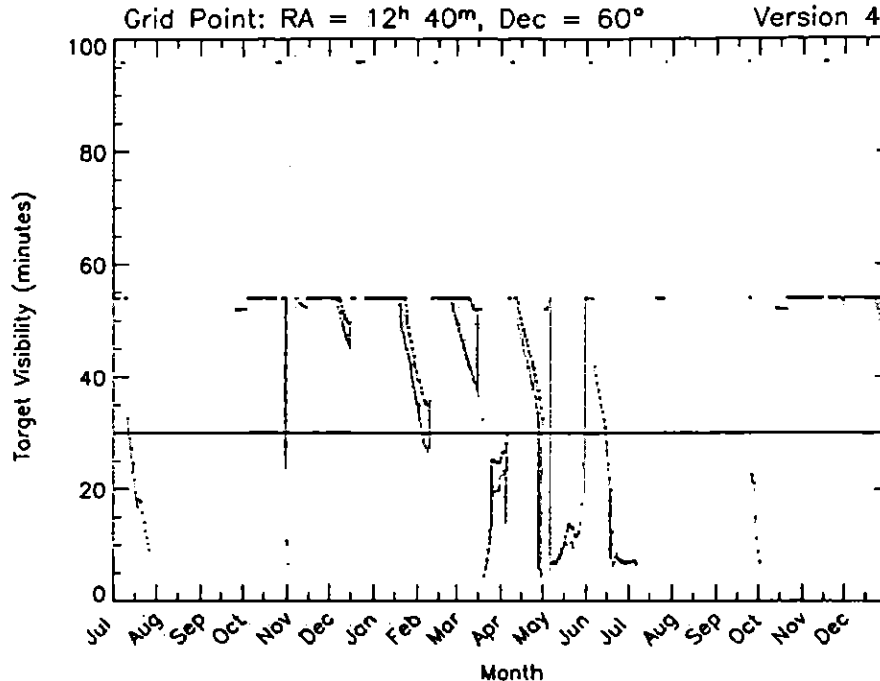
In this section we provide some examples of how to determine the schedulability and visibility period for different types of observations in two-gyro mode.

2.3.4 Examples

Orbit	Year 2007											
	Aug 15	Aug 16	Aug 17	Aug 18	Aug 19	Aug 20	Aug 21	Aug 22	Aug 23	Aug 24	Aug 25	
270	0	0	0	0	0	0	0	0	0	0	0	54
269	0	0	0	0	0	0	52	54	54	54	54	
268	0	0	0	53	53	52	52	54	54	54	54	
267	53	53	53	53	53	52	52	54	54	54	54	
266	53	53	53	53	53	51	51	54	54	54	54	
:	:	:	:	:	:	:	:	:	:	:	:	
235	53	53	53	53	53	53	44	45	45	0	51	
227	53	53	53	53	53	40	40	41	42	43	44	
226	53	53	53	53	53	40	40	41	42	43	44	
225	0	0	0	53	53	39	40	40	41	41	44	
224	0	0	0	0	0	0	39	40	41	42	43	
223	0	0	0	0	0	0	0	0	0	42	43	
222	0	0	0	0	0	0	0	0	0	41	43	

Table 2.5: A portion of the Tabular Output for the Data Shown in Figure 2.10

Figure 2.11: Time Available per Orbit for the HDF in Cycle 15



Let's consider first the HDF. Using the on-line tool available at the Two-Gyro Science web site, we examine the scheduling and visibility plots available for the $\alpha = 12^{\text{h}} 40^{\text{m}}$, $\delta = 60^{\circ}$ grid point. The plot of number of available days versus orientation shows that there are many days in Cycle 15 that the HDF is observable in two-gyro mode provided that the orientation is greater than ~ 130 degrees. Since Observer #1 does not have an orientation constraint, we skip the plot of orientation versus month and proceed directly to the plot of visibility versus month. From this plot (Figure 2.11), we see that good visibility is achievable for this program throughout much of the year.

This program could be conducted with a set of 4 observing opportunities spaced ~ 45 days apart (e.g., 01-Oct-2006, 14-Nov-2006, 29-Dec-2006, 12-Feb-2007). The science times available per orbit on these dates are listed in Table 2.6. A larger set of observations may be difficult to schedule since the next opportunity in this set (March 29) has very poor visibility. When dealing with visibilities that change rapidly over the course of a month, flexibility in time series spacing may improve the schedulability. For example, in this case allowing a 55 day separation from February 12 to April 8, instead of the 45 day spacing between February 12 and March 29, would increase the visibility sufficiently to make another epoch of observations possible.

Now consider the HUDF. Using the on-line tool available at the Two-Gyro Science web site, we examine the scheduling and visibility plots available for the $a = 3$ 40m, $\delta = -30^\circ$ grid point. The possibilities for scheduling a series of observations with a spacing of 45 days is more limited due to the gap from mid-December 2006 to June 2007. Starting the series as early as possible is the only way to obtain four observing opportunities.

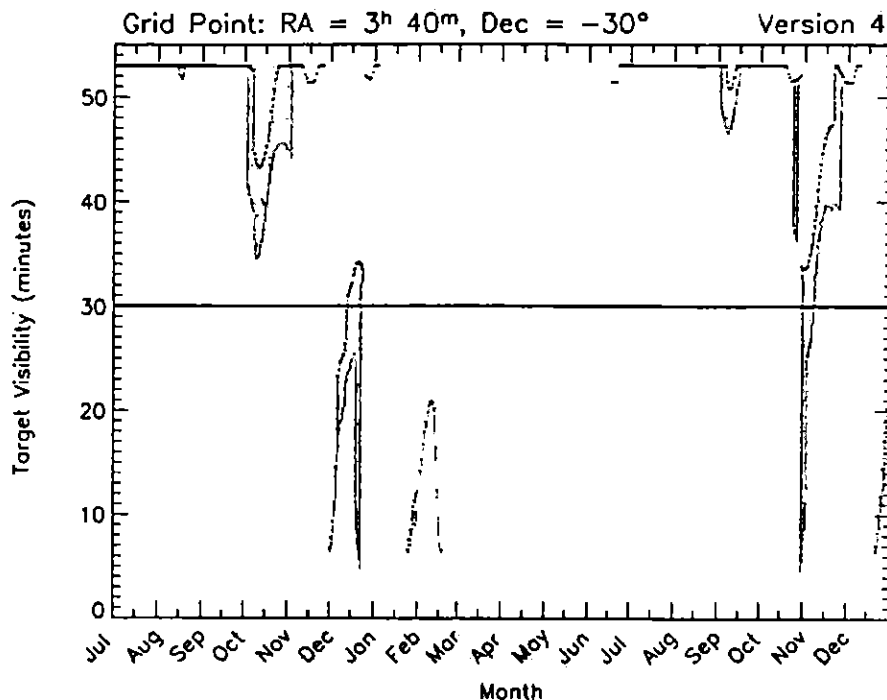
Table 2.7: Two-Gyro Time for the HUDF on Selected Dates in Cycle 15

Observation Date	Time per Orbit (minutes)
01-Jul-2006	53
14-Aug-2006	53
28-Sep-2006	57
12-Nov-2006	52

Table 2.6: Two-Gyro Time for the HDF on Selected Dates in Cycle 15

Observation Date	Time per Orbit (minutes)
01-Oct-2006	52
13-Nov-2006	53
14-Nov-2006	52
15-Nov-2006	54
28-Dec-2006	54
29-Dec-2006	54
30-Dec-2006	54
11-Feb-2007	54
12-Feb-2007	54
13-Feb-2007	96
28-Mar-2007	25
29-Mar-2007	25
30-Mar-2007	25

Figure 2.12: Time Available per Orbit for the HUDF in Cycle 15



Example 2: Time-series light curve observations of a supernova found in Example 1.

Observer #1 finds a supernova in the HDF using the experiment outlined in Example 1 and wants to obtain the light curve of the supernova by obtaining photometric images of the supernova and surrounding field once a week for 7 weeks. The supernova was discovered after the fourth set of observations was obtained on 12 February 2007.

Using the visibility versus month plot generated for Example 1, Observer #1 notes that the orbital visibilities for the HDF and surrounding areas are good on February 19 and 26 (54 minutes) as well as March 5 and 12 (54 and 53 min, respectively). However, by March 19 the visibility has dropped to 33 minutes, and by March 26 it is only 25 minutes. Thus, it is not possible to follow the supernova light curve throughout the entire 45 day period as hoped.

If the supernova had been found after the second epoch observations of the HUDF (instead of the HDF), it would have been possible to follow the light curve for the full 45 day interval between 14 August 2006 and 2 October 2006 (see Figure 2.12).

Example 3: Time-constrained observations of recurrent nova T Pyx.

Examination of this plot provides the following information (assuming a 9 October 2006 start) for the relative timing of the observations and the amount of science time available per orbit.

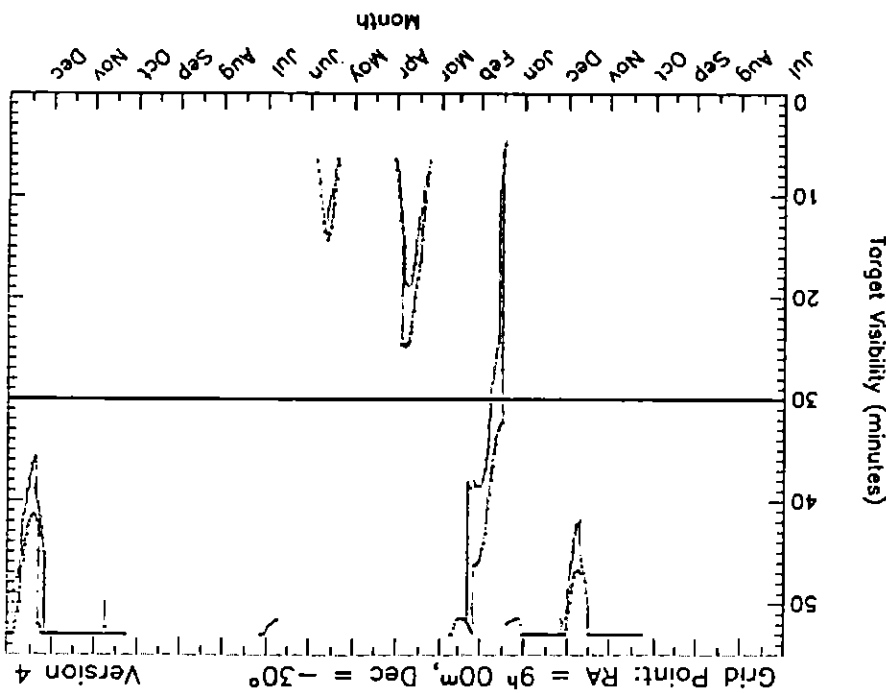


Figure 2.13: Time Available for T_{PYX} in Cycle 15

Observer #3 wants to observe the recurrent nova T_{PYX} ($\alpha = 9^{\circ} 05m$, $\delta = -32^{\circ} 23'$) during its next outburst, which should begin in early October 2006. The objective is to study the evolution of the ejected shell using images (3 orbits with at least 46 minutes of visibility) obtained as soon as possible after outburst, followed by images 7, 21, 49, 84, 112, 140, and 365 days later. There are no orientation constraints on the observations. Observer #3 estimates the science time available using the nearby position at $\alpha = 9^{\circ} 0m$, $\delta = -30^{\circ}$ (see also Table 2.8).

Table 2.8: Two-Gyro Time Available for T Pyx on Selected Cycle 15 Dates

Observation Date	Relative Timing (days)	Time per Orbit (minutes)
09-Oct-2006	0	53
16-Oct-2006	7	53
30-Oct-2006	21	53
27-Nov-2006	49	48
01-Jan-2007	84	53
29-Jan-2007	112	44
26-Feb-2007	140	0
09-Oct-2007	365	53

Two of the observations have less than the 46 minutes of visibility needed for this particular science investigation, and are therefore not suitable choices for this time series. The day 112 observation would need to be moved back to February 3, while the day 140 observation would need to be moved to February 22. Since these observations have moved closer together, Observer #3 decides to drop the day 140 observation. A possible revised series of observations is given in Table 2.9.

Table 2.9: Revised Two-Gyro Time Series for T Pyx in Cycle 15

Observation Date	Relative Timing (days)	Time per Orbit (minutes)
09-Oct-2006	0	53
16-Oct-2006	7	53
30-Oct-2006	21	53
27-Nov-2006	49	48
03-Feb-2007	117	46
09-Oct-2007	365	51

However, while the outburst is expected around the beginning of October, it could occur later in the month, so it is necessary to check how a later outburst would impact the observations. With start dates of October 16, 23, and 30, the following sequences listed in Table 2.10 are possible. Thus, if T Pyx goes into outburst anytime in October, the observations can be successfully obtained in two-gyro mode.

Observer #4 wants to take an ACS image of a portion of the Vela supernova remnant near the position of the star HD 72089 ($\alpha = 08^{\text{h}} 29^{\text{m}}, \delta = -45^{\circ} 33'$). A roll angle of 70 ± 5 degrees must be used to keep the bright star off the detector. A second observation to observe a different part of the web yields the following plots of the number of days each orientation is available (Figure 2.14) and orientation versus month (Figure 2.15) for the checks the availability of orientations 180 degrees from those originally envisaged. The inverse orientations at 250 degrees and 340 degrees are accessible in October 2006 and December 2006, respectively. Therefore, this observation is feasible in two-gyro mode as long as the requested orientations are changed to 250 ± 5 degrees and 340 degrees. The availability of allowable orientations must be described appropriately in the Phase I proposal.

Realizing that the planned orientations are not viable, Observer #4

time in Cycle 15.

an orientation of 70 degrees cannot be achieved in two-gyro mode at any nearby position at $\alpha = 8^{\text{h}} 20^{\text{m}}, \delta = -45^{\circ}$. It is apparent from these plots that an orientation of 70 ± 5 degrees cannot be achieved in two-gyro mode at any nearby position at $\alpha = 8^{\text{h}} 20^{\text{m}}, \delta = -45^{\circ}$. It is apparent from these plots that an orientation of 70 degrees cannot be achieved in two-gyro mode at any

available (Figure 2.14) and orientation versus month (Figure 2.15) for the web yields the following plots of the number of days each orientation is available (Figure 2.14) and orientation versus month (Figure 2.15) for the checks the availability of orientations 180 degrees from those originally envisaged. The inverse orientations at 250 degrees and 340 degrees are accessible in October 2006 and December 2006, respectively. Therefore,

Example 4: An orientation-constrained observation of the Vela supernova remnant.

Observation	Time per Orbit (minutes)	Observation Per Orbit (minutes)	Date/Timing	Observation Per Orbit (minutes)	Date/Timing	Time per Orbit (minutes)
16-Oct-2006 / 0	53	23-Oct-2006 / 0	53	30-Oct-2006 / 0	53	53
23-Oct-2006 / 7	53	30-Oct-2006 / 7	53	06-Nov-2006 / 7	53	53
06-Nov-2006 / 21	53	13-Nov-2006 / 21	53	20-Nov-2006 / 21	47	53
04-Dec-2006 / 49	53	11-Dec-2006 / 49	53	18-Dec-2006 / 49	53	53
08-Jan-2007 / 84	52	52
05-Feb-2007 / 112	46	12-Feb-2007 / 112	52	19-Feb-2007 / 112	52	53
16-Oct-2007 / 365	53	23-Oct-2007 / 365	53	30-Oct-2007 / 365	53	53

Table 2.10: Alternative Time Series for T Pyx in Cycle 15

Figure 2.14: Cycle 15 Orientation Availability in the Direction of the Vela SNR

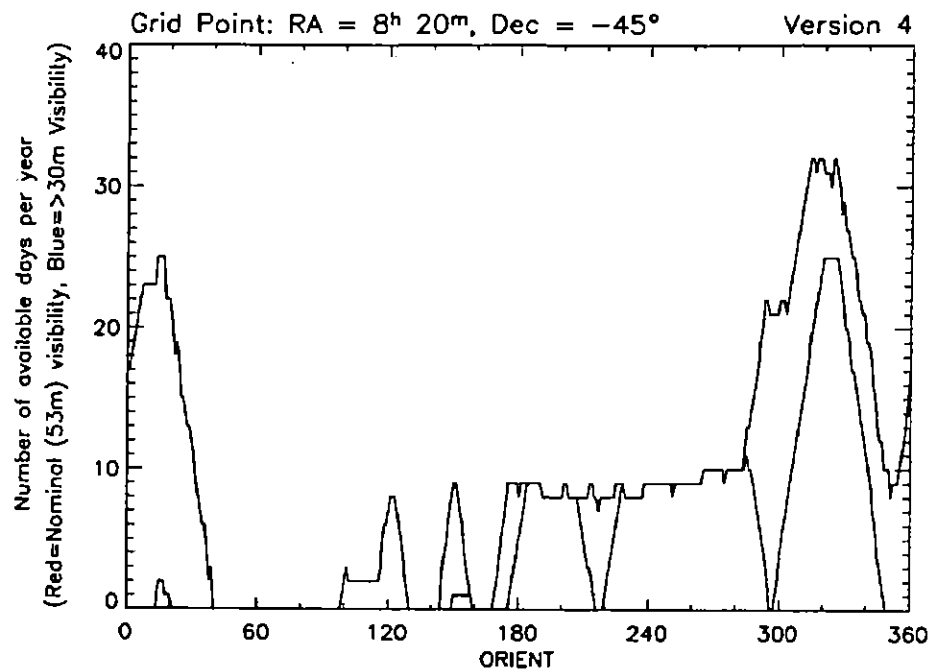
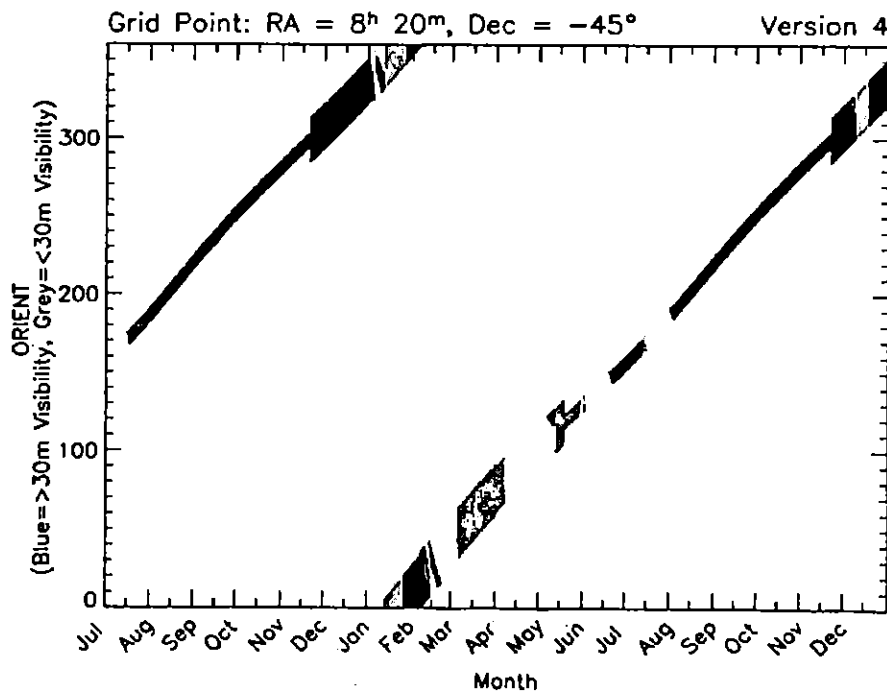


Figure 2.15: Cycle 15 Orientation Angles Versus Month Toward the Vela SNR



orbital visibility is 96 minutes should be considered CVZ candidates. Plots, like those discussed above. Only those observations for which the quality for CVZ time, observers should consult the visibility tables and constraints. To determine whether constrained two-gyro observations mode, but the durations may be shorter because of more restrictive pointing constraints.

The CVZs in two-gyro mode will be the same size as those in three-gyro

orbits (see Section 2.3.2 in the *HST Primer*).

Crossings limit the uninterrupted visibility of any target to no more than 5–6 hours by Sun and Earth limb avoidance. South Atlantic Anomaly imposes upon the telescope orbit, target position, and constraints duration depends upon the orbital precession cycle. The CVZ at some time during the 56-day HST orbital precession cycle. The CVZ located in declination bands near $\pm 61.5^\circ$ degrees may be in the CVZ at some orbital poles, which are 28.5° degrees from the celestial poles. Thus, targets HST can observe without interruptions caused by target occultation by the Earth. These zones are approximately 24° degrees in size centred on the HST can observe without interruptions caused by target occultation by the

CVZs are regions of the sky where HST can observe without interruptions caused by target occultation by the

2.6 Continuous Viewing Zones

The continuous viewing zones (CVZs) are regions of the sky where HST can observe without interruptions caused by target occultation by the Earth. These zones are approximately 24° degrees in size centred on the HST can observe without interruptions caused by target occultation by the CVZs are regions of the sky where HST can observe without interruptions caused by target occultation by the

2.5 Two-Gyro Orbit Calculations for Phase I

The visibility period for two-gyro observations should make use of the two-gyro visibility periods from the plots and tables described in this chapter. The tools for creating these plots and tables are available on the Two-Gyro Science Mode web site. Exposure times for two-gyro observations should be calculated with the appropriate two-gyro exposure time calculators (ETCs) for each instrument. In most cases, these are the same ETCs as were used for three-gyro mode since the instruments performance in both cases is nearly indistinguishable. Links to these ETCs can be found on the main web page for each instrument.

2.4 Verifying Scheduling Constraints for Phase I

2.7 Moving Targets

We expect that there will be no significant impact of two-gyro operations on moving target observations other than that gyro-only tracking and guide star handoffs are not available in two-gyro mode. Proposers wanting to observe moving targets should consult the Two-Gyro Science Mode web page for updates, which will be posted as information about observing moving targets in two-gyro mode becomes available.

CHAPTER 3:

The HST Gyroscopes

In this Chapter...

3.1 Gyroscope Overview / 33

3.2 Previous Gyroscope Replacements / 36

3.1 Gyroscope Overview¹

HST has six rate-sensing gyroscopes. Two of the six gyroscopes are no longer functioning. Under normal operating procedures, three of the six gyros must be functioning to provide sufficiently accurate pointing to achieve guide star acquisitions and science data collection. The gyroscopes aboard HST sense whenever the attitude of the observatory is changing, whether during large angle slews from one target to another or during small pointing changes as a result of subtle forces acting upon the observatory. Each gyroscope senses the motion about a single axis. The relative orientations of the gyro axes within HST are different so that the torques exerted on the gyroscopes by attitude changes affect each gyro differently. As a result, any combination of three gyros can be used to define a set of three orthogonal axes around which changes in the roll, pitch, and yaw of the observatory may be measured.

There are many different types of gyroscopes available, but only gas bearing gyros are capable of providing the combination of extremely low noise, excellent stability, and high sensitivity to motions that is required for HST observations. Each gyro has a wheel spinning at a constant rate of 19,200 rotations per minute on gas bearings. The wheel is mounted in a sealed cylinder, which floats in a thick fluid. Electricity is carried to the motor that spins this wheel by thin wires, or flex leads, approximately the

1. Some of the information in this chapter was reproduced from the *Hubble Space Telescope Gyroscopes Hubble Facts sheet* available from the GSFC HST Program Office.

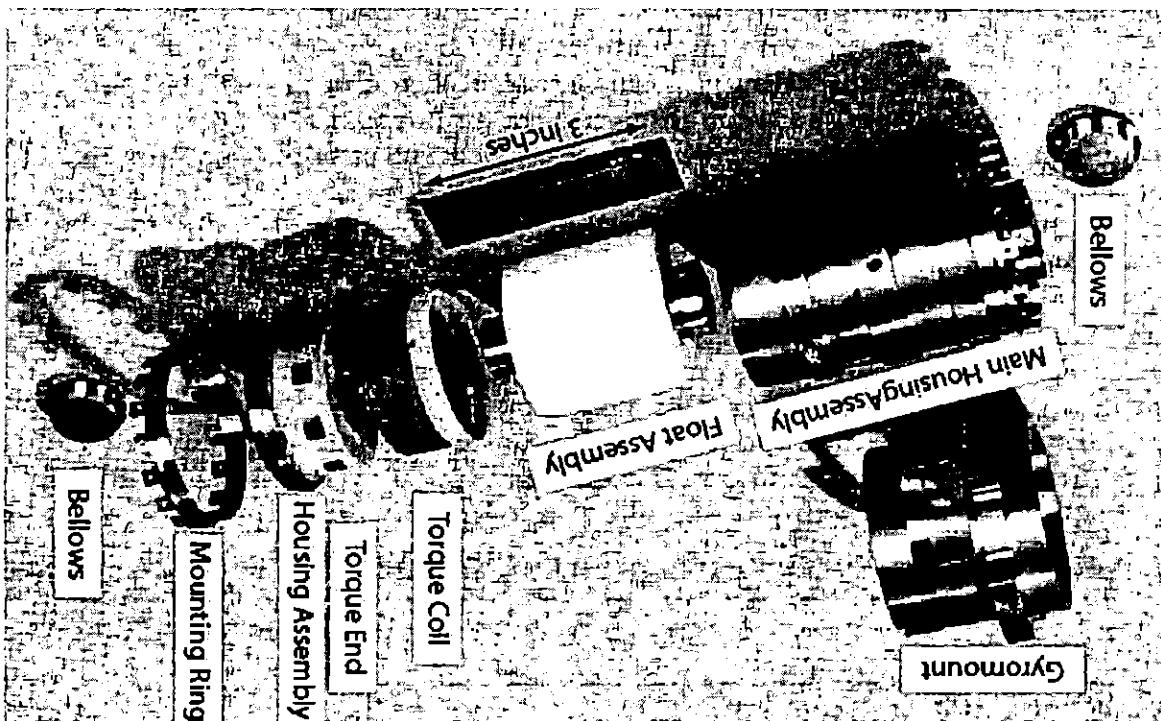


Figure 3.1: Exploded View of a Gas Bearing Gyroscope

The gyroscopes are packaged in pairs, in devices called rate sensing units (RSUs). Each RSU weighs approximately 24.3 pounds and is 12.8 x 10.5 x 8.9 inches in size. The individual gyroscopes weigh approximately 6 pounds and are 2.75 x 6.5 inches in size. Figure 3.1 shows an exploded view of one of the HST gyroscopes. Figure 3.2 shows a gyro assembly.

Figure 3.2 shows a gyro assembly. The assembly consists of a central computer where it is analyzed. The HST pointing is changed through the use of several reaction wheels. Each assembly contains spinning wheels, which when spun at varying rates, create the appropriate torque required for the desired movement.

Changes in the gyroscope rates induced by movement of HST are captured by onboard electronics. This information is then fed to Hubble's central computer where it is analyzed. The HST pointing is changed through the use of several reaction wheels. Each assembly contains spinning wheels, which when spun at varying rates, create the appropriate torque required for the desired movement.

Figure 3.2: Assembled Gyroscope

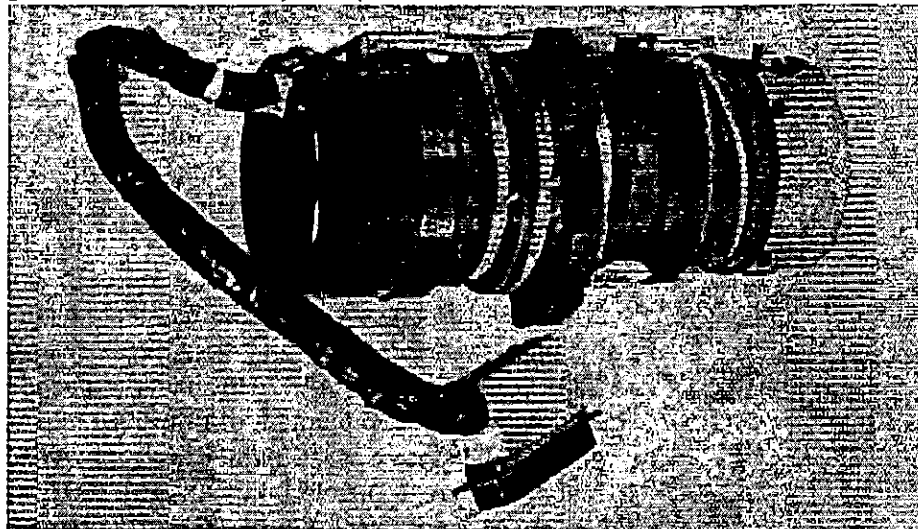
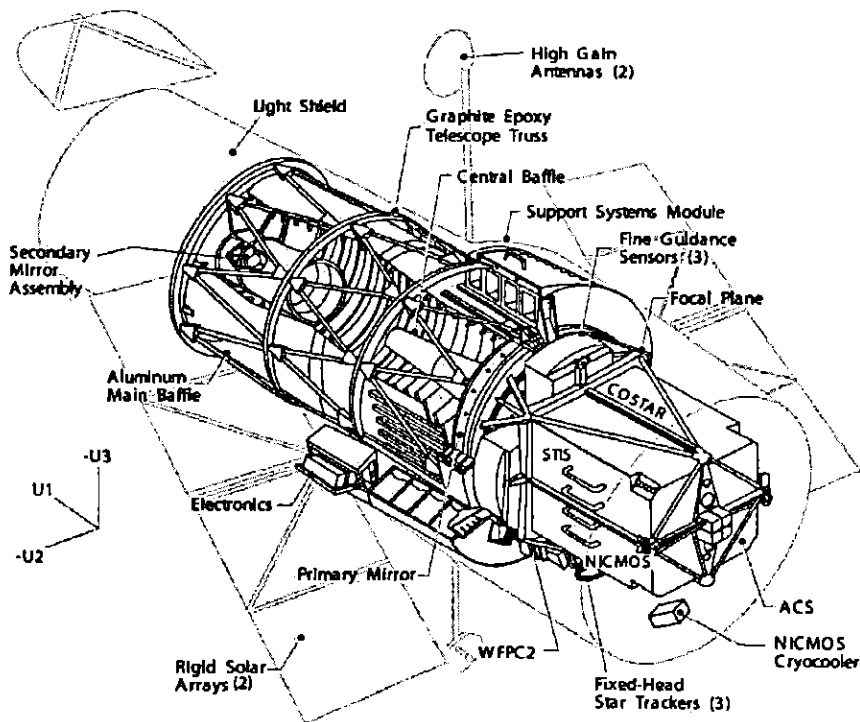


Figure 3.3: Schematic of the Hubble Space Telescope after Servicing Mission 3B



Major components are labelled, and definitions of the U1, -U2, -U3 (V1, V2, V3) space-craft axes are indicated.

The HST gyroscopes are attached to the focal plane structure at the aft end of the observatory on the same side as the fixed-head star trackers (FHSTs). Figure 3.3 shows the HST field of view following SM3B in the standard HST coordinate system. The RSUs are accessed by opening the large cargo bay doors on the U3 side of the observatory.

Four of the six original HST gyroscopes were replaced during the first servicing mission (SM1) in December 1993 by astronauts aboard Space Shuttle flight STS-61. In the years after this servicing mission, the HST gyroscopes failed at a higher-than-expected rate. On 13 November 1999, gyroscopes failed at a higher-than-expected rate. On 13 November 1999, the fourth of six gyroscopes aboard HST failed, leading to a halt of science observations and entry into safe mode. In anticipation of this event, NASA had been planning for several years, splitting into two separate missions: SM3A and SM3B. During SM3A servicing mission 3, which NASA had been planning for several years, the four gyroscopes aboard HST failed, leading to a halt of science observations and entry into safe mode. In anticipation of this event, three gyroscopes (#1 and #2) currently providing attitude control in two-gyro RSUs (STS-103, December 1999), astronauts replaced all six gyroscopes (three gyroscopes (#1 and #2) currently providing attitude control in two-gyro RSUs). The first gyroscopes (Gyro #5) failed on 28 April 2001, and the second (Gyro #3) failed on 29 April 2003. Gyros #6 and #4 have been turned off to extend their lifetime; one will be switched back on when one of the two gyroscopes fails.

In the time since SM3A, two of the six gyroscopes have failed. The first gyroscopes (Gyro #5) failed on 28 April 2001, and the second (Gyro #3) failed on 29 April 2003. Gyros #6 and #4 have been turned off to extend their lifetime; one will be switched back on when one of the two gyroscopes fails. The first gyroscopes (Gyro #5) failed on 28 April 2001, and the second (Gyro #3) failed on 29 April 2003. Gyros #6 and #4 have been turned off to extend their lifetime; one will be switched back on when one of the two gyroscopes fails.

3.2 Previous Gyroscope Replacements

CHAPTER 4:

Slewing and Pointing

In this chapter . . .

4.1 Overview / 37
4.2 Two-Gyro Coordinate Conventions / 38
4.3 Pointing Control with Two Gyros / 39
4.4 Pointing Constraints / 43

4.1 Overview

Slewing of HST is much the same in two-gyro mode as in three-gyro mode, with a few important differences. The primary difference between the two modes is the accuracy of the pointing at the ends of slews. In three-gyro mode, the telescope is generally pointed to within 50-100 arcseconds of the target after a 180 degree slew. In two-gyro mode, the pointing error at the end of a slew of any duration can be as large as 10 degrees because the rate change for one axis of control must be supplied by the HST magnetometers rather than by a gyroscope. For this reason, it is necessary to have a different sequence of activities at the ends of slews in two-gyro mode.

The slew rates in two-gyro and three-gyro modes differ slightly. In three-gyro mode, the maximum maneuver rate is ~11 degrees per minute of time with a typical rate of ~6 degrees per minute. In two-gyro mode the maneuver rate is expected to be ~85% of these values. Two-gyro pointing control and constraints are described in the following sections.

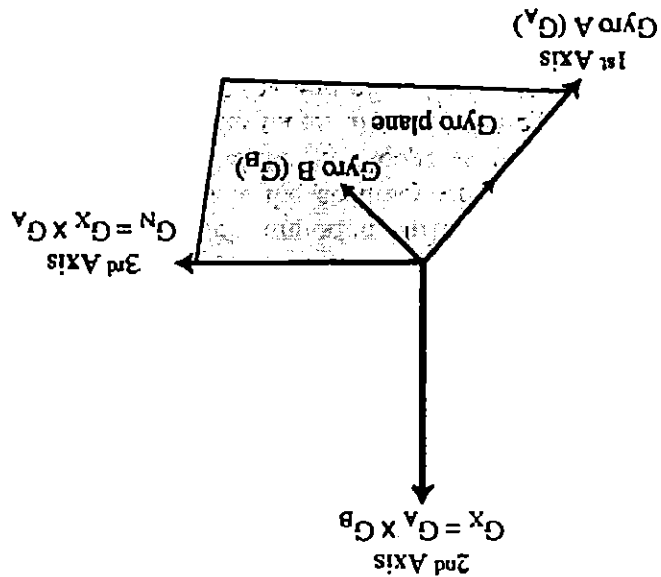


Figure 4.1: Orthogonal Two-Gyro Coordinate System

To more easily understand the control of the telescope with two gyros, it is convenient to define a reference frame for the gyroscope control directions and the "missing" control axis. Figure 4.1 is an illustration of an orthogonal coordinate system with two gyros (Gyro A and Gyro B). The first axis of the system is defined by the Gyro A measurement axis. The second axis is defined by the cross product of the two measurement axes of Gyro A and Gyro B. This axis is called the G_x axis. The semi-major axis of the jitter ellipse is the direction associated with rotations about the G_x axis. The information for the G_x axis must be supplied by one of the HST pointing control system sensors other than the two functioning gyros, such as the Fine Guidance Sensors. The third axis is defined by the cross product of the second (G_x) and first (G_A) axes. This axis lies in the gyro plane in a direction that is 90° from the G_A axis.

4.2 TWO-GYRO COORDINATE CONVENTIONS

4.3 Pointing Control with Two Gyros

A major rework of the HST attitude control software was necessary to prepare HST for two-gyro operations. This extensive redesign was done by engineers and software experts at the Goddard Space Flight Center. The various control modes described below are part of the updated onboard attitude control system and are invoked automatically when needed.

4.3.1 Magnetic Sensing System and Two Gyros (M2G)

The M2G mode uses two gyros in combination with information about the Earth's magnetic field orientation to provide pointing control. The Magnetic Sensing System (MSS) on HST consists of two magnetometers. The magnetometers measure the strength and direction of the Earth's magnetic field. Together with a model for the magnetic field, they can be used to supply pointing control information for the G_x axis. The typical pointing accuracy in M2G mode is 2-5 degrees but can be as poor as ~10 degrees when the G_x axis is aligned with the Earth's magnetic field. This mode is used during large-angle slews and FHST and FGS occultations. It may also be entered when onboard attitude determinations (OBADs) fail, as guide star acquisitions will not be attempted.

Attitude is estimated in M2G mode through a combination of rates provided by the two gyros and the attitude derived from the cross product of the magnetic field model and the magnetic field measured by the MSS. The time derivative of the magnetic field is measured in the vehicle reference frame by the MSS. The data for this magnetic field change is filtered heavily before comparison to the expected value of the magnetic field derivative calculated from the magnetic field model. The difference between the measured and predicted values reveals the magnitude of pointing inaccuracies if the alignment of HST with the Earth's magnetic field is favorable for such comparisons.

M2G mode has the following sub-modes:

1. *Attitude Hold Mode*: This mode is used when gyro plane errors are expected to be small (e.g., after two successful onboard attitude determinations). The G_x axis is controlled by the MSS, while the gyro plane is controlled with the gyro rate information. This mode can be entered from the T2G mode after a successful OBAD.
2. *Maneuver Mode*: This mode is used to perform large-angle vehicle maneuvers. The G_x axis is controlled by the MSS, while the gyro plane is controlled with the gyro rate information in conjunction with additional information from the MSS. This mode can be entered only from the M2G attitude hold or M2G coarse attitude hold modes.

- The T2G mode uses two gyros in combination with one or more of the fixed-head star trackers to provide pointing control necessary to perform attitude determinations and to reduce the pointing uncertainty to less than 1 arc minute. HST has three HHTSs that are located at the aft end of the observatory. They are attached to the focal plane structure close to the gyroscopes. One HHTS points along the $-V_3$ axis. The other two are tipped backwards and tilted relative to the $-V_1$ direction, pointing toward the rear of the observatory. The HHTSs have 8×8 degree fields of view and are sensitive to stars brighter than $m_V \sim 6$, with a typical centroiding accuracy of 10-15 arcseconds. The use of HHTS information is required throughout the T2G mode.
- Upon entering T2G mode from M2G mode, an HHTS is used to lock onto the position of any star, and this information is fed into the control law and while the vehicle rates about the G_X axis. After the rates have damped to damp the vehicle rates about the G_X axis, a second HHTS can be used to collect information about the star positions in its field of view. The star maps are compared to an onboard star catalog to determine the attitude of the observatory. This onboard attitude determination may be followed by a maneuver to correct the pointing, and a second OBAD is performed to ensure that the pointing has been refined sufficiently.
- The rate damping in T2G mode following an M2G mode sequence is expected to take less than ~120 seconds. The attitude error following small (~ 0.5 degree) maneuvers is expected to be ≤ 15 arcseconds. The attitude error following an extended period of attitude hold is expected to be ≤ 30 arcseconds.
1. Rate Damping Mode: This mode uses information from the HHTSs to damp the rates and to provide pointing stability in the G_X axis. It is mode that can be entered from zero gyro support (ZGSP) safe mode.
2. Attitude Hold Mode: This mode determines and holds the observatory attitude after the rates have been damped. One or more OBAs with the HHTSs may occur while in this mode. It is the sole entry point into the F2G mode. It can be entered from the T2G rate damping mode that can be entered from zero gyro support (ZGSP) safe mode.
3. Coarse Attitude Hold Mode: This mode is used when significant gyro plane errors are expected (e.g., after an onboard attitude determination failure). The G_X axis is controlled by the MSS, while the gyro plane is controlled with the gyro rate information in conjunction with additional information from the MSS. This mode can be entered from the M2G maneuver mode or from the T2G mode after an unsuccessful OBAD.

mode or from the F2G mode. It can also be re-entered from the T2G maneuver mode after a vehicle maneuver.

3. *Maneuver Mode*: This mode is used to perform the maneuvers required for attitude corrections following an OBAD in the T2G attitude hold mode. After the maneuver, control is returned to the T2G attitude hold mode.

4.3.3 Fine Guidance Sensors and Two Gyros (F2G)

The F2G mode uses information from the HST FGSs in combination with two gyros to provide the fine pointing control required for guide star acquisitions and science observations. Just before entering F2G mode, an FGS is used to find and track a star. Upon entering F2G mode, the FGS is used in coarse track mode to control the attitude along the G_X axis and dampen the rates remaining from the T2G activities. A second FGS then searches for a guide star, enters coarse track mode, and proceeds to fine lock. Once in fine lock, it provides information for the G_X axis. After the jitter is low enough, the first FGS transitions into fine lock and reduces the jitter even further so that the guide star acquisition and science observations can be performed.

The F2G mode has two sub-modes:

1. *F2G-CT*: This is the F2G coarse track mode. This mode is used to damp the gyro rates remaining from T2G mode in preparation for entry into F2G fine lock mode.
2. *F2G-FL*: This is the F2G fine lock mode. Science observations are obtained in this mode after the guide star acquisition is completed. The jitter in this mode is comparable to the jitter observed in three-gyro mode. Control in this mode is performed using the dominant (brighter) guide star.

An abort from either F2G sub-mode results in the attitude control system dropping back into T2G mode. From here, it may be necessary to drop into M2G mode if FHST visibility is insufficient to remain in T2G mode.

4.3.4 A Typical Sequence of Events for an Acquisition

The general sequence of events that must occur for an HST science observation to be made (slew, guide star acquisition, and science observation) are the same in three-gyro mode and two-gyro mode, but the implementation of these events is considerably different. Figure 4.2 depicts these events in graphical form. The sequence for both modes begins with a slew to the target.

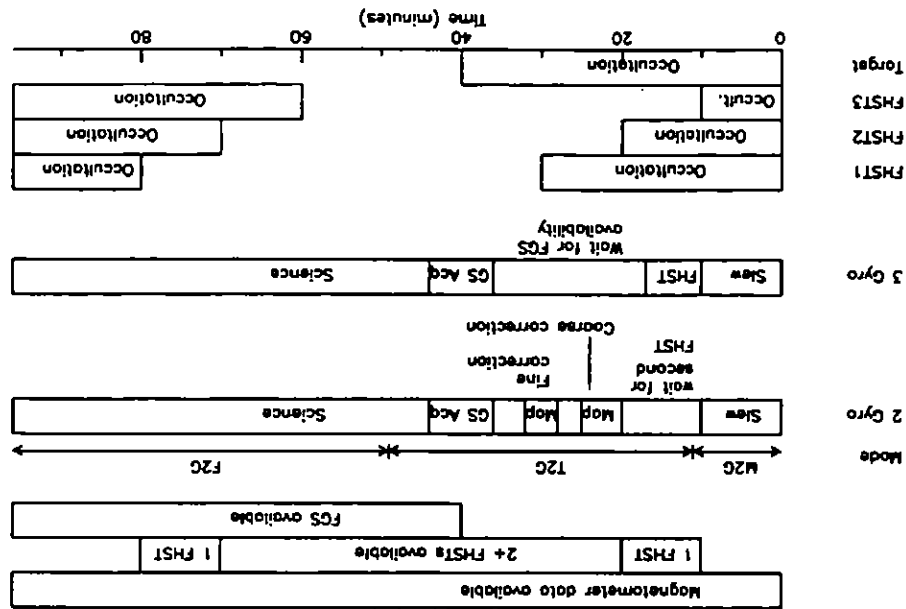


Figure 4.2: Typical Sequence of Events for an Observation

In two-gyro mode, the slew is performed in M2G mode under the control of two gyros and the MSS. T2G mode is entered when an FHT occurs, the FHTs are used to locate stars for an onboard attitude determination and to correct the pointing, which may be off by as much as 10 degrees. (OBDs are indicated by the "map" blocks in Figure 4.2.) A second OBD is required to check the correction, and this information is used to refine the pointing even further. While waiting for the FGs to become unocculted, the FHTs are used to stabilize the pointing. When an FGs is available, the guide star acquisition process commences and F2G mode is entered to reduce the pointing uncertainties and jitter even further. The science observation begins at the end of the guide star acquisition. During occultation the control system drops back to M2G mode, and the whole process, from M2G through F2G, must be repeated for the next orbit.

In three-gyro mode, the slew is performed in M2G mode under the observation. In the end of the slew and the start of the guide star acquisition process, the gyros update any FHT and can occur at any point before the acquisition. When the FGs come out of occultation, the guide star acquisition occurs and is followed immediately by the science acquisition (s), which may include a target acquisition. The science observation can continue until the target is occulted. During occultation, the telescope pointing drifts by less than ~ 5 arcseconds. On subsequent orbits, a guide star re-acquisition occurs and is followed by another science observation.

4.3.5 Gyro-only Pointing

Observing without the use of guide stars (gyro-only pointing) is occasionally allowed in three-gyro mode (see Section 3.2.3 of the *HST Primer*). In two-gyro mode, gyro-only pointing is not allowed for external science observations. It may still be used for external Earth-calibration exposures or internal calibration exposures.

4.4 Pointing Constraints

The need to use a sequence of MSS, FHSTs, and FGS observations to provide attitude control information for the G_X axis in two-gyro mode results in a set of pointing constraints that is more stringent than in three-gyro mode. The pointing uncertainty of as much as 10 degrees in M2G mode requires more stringent Sun-avoidance constraints. The need to have FHST coverage throughout T2G mode also results in reduced scheduling possibilities since multiple FHSTs must be unocculted by the Earth at the appropriate times. This latter constraint is the primary reason for the reduced schedulability of targets in directions ahead of the Sun (see Chapter 2). A summary of pointing constraints in both three-gyro mode and two-gyro mode is provided in Table 4.1.

Table 4.1: Pointing Constraints Summary

Pointing Constraint	Three-Gyro Mode	Two-Gyro Mode
Sun angle range allowed	50°-180°	60°-180°
Off-nominal roll angle allowed	5° for V1-Sun angle 50°-90°; increasing to 30° at V1-Sun angle = 178°; unlimited at V1-Sun-angle = 178°-180°	5° for V1-Sun angle 60°-115°; increasing to 20° at V1-Sun angle = 179°; unlimited at V1-Sun-angle = 179°-180°
V1 Moon constraint (FGS HV on)	>9.5°	Same as three-gyro mode
Earth avoidance (FGS guiding, dark limb)	>6°	Same as three-gyro mode
Earth avoidance (Science obs, dark limb)	>6°	Same as three-gyro mode
Earth avoidance (FGS guiding, bright limb)	>13.5°	Same as three-gyro mode
Earth avoidance (Science obs, bright limb)	>20°	Same as three-gyro mode
SAA avoidance	Instrument dependent	Same as three-gyro mode

CHAPTER 5:

Guiding and Jitter

In this chapter . . .

5.1 Guiding / 45
5.2 Jitter Overview / 48
5.3 Disturbances and Primary Sources of Jitter / 51
5.4 HSTSIM Jitter Simulations / 54

5.1 Guiding

The general procedures for acquiring guide stars in preparation for science observations are outlined in the *Slewing and Pointing* chapter of this Handbook. Here, we concentrate on a few key issues that are relevant for guiding while science observations are taking place.

5.1.1 Guide Star Acquisitions

Guide star acquisitions in two-gyro mode take the same amount of time as those routinely performed in three-gyro mode (~6 minutes). Unlike three-gyro mode, however, the pointing errors accumulated during occultations by the Earth in two-gyro mode are expected to be sufficiently large to prevent the types of guide star re-acquisitions that are currently performed in three-gyro mode. Therefore, full guide star acquisitions are performed every orbit in two-gyro mode.

Single guide star acquisitions have sometimes been necessary when two suitable guide stars could not be acquired by the FGSs. While this type of acquisition is possible in three-gyro mode, single guide star acquisitions are not allowed in two-gyro mode. If a pair of suitable guide stars cannot be acquired in two-gyro mode during the guide star acquisition, the pointing control system will drop into a coarser pointing mode (see Section 4.3).

Unlike three-gyro mode, pointing performance and maintenance of guide star lock in two-gyro mode depended on the magnitudes of the guide stars chosen. Figure 5.1 shows a histogram of the magnitudes of all guide stars used by HST from January 2000 through August 2004. The average magnitude of $M_V = 12.3$. These estimates include magnitudes for both guide star magnitude in this time period was $M_V = 12.1$, with a median magnitude of $M_V = 11.3$, and 25% were fainter than $M_V \geq 14.0$. Chapter 7 contains additional information about the brightness distribution of the guide stars for each FGS in this time period.

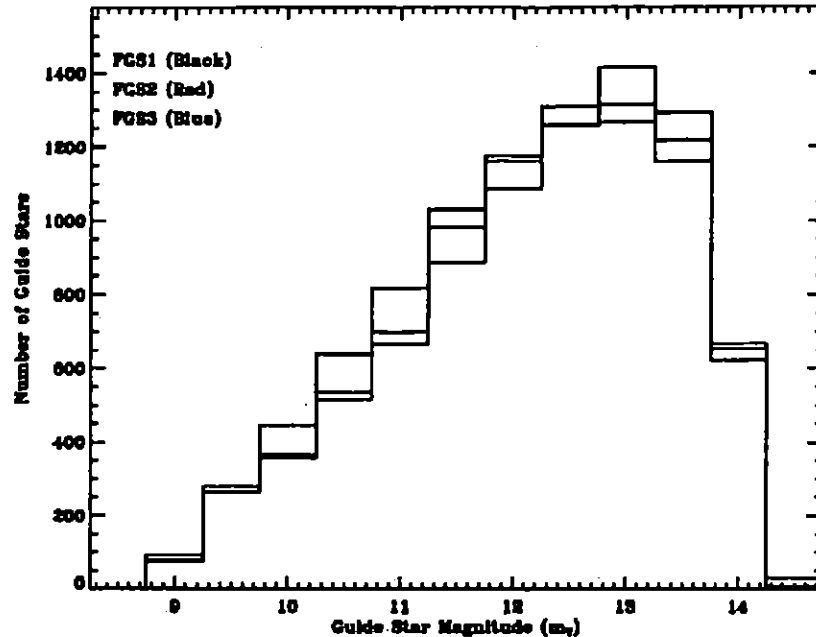
5.1.2 Guide Star Magnitudes

Activity	Two-Gyro Mode	Three-Gyro Mode	Observation proceeds successfully acquired with only 1 star successfully acquired Acquisition fails; revert to T2G or proceeds success- fully in many cases	Dual guide star acquisition with only 1 star successfully acquired Acquisition fails; revert to T2G or M2G mode
Single guide star acquisition	Not Allowed	Allowed		
Guide star acquisition (orbits following initial orbit in visit) (re-acquisition)	~6 min	~5 min		
Guide star acquisition (initial orbit in visit)	~6 min	~6 min		
			With only 1 star successfully acquired Acquisition fails; revert to T2G or proceeds success- fully in many cases	

Table 5.1: Guide Star Acquisitions

Table 5.1 summarizes some of the relevant guide star acquisition differences between three-gyro and two-gyro mode.

Figure 5.1: HST Guide Star Magnitudes (Jan. 2000 - Aug. 2004)



5.1.3 Guiding Performance

On-orbit tests in February 2005 showed that the guiding performance in two-gyro mode (F2G-FL) is similar to the guiding performance in three-gyro mode. Additional tests are planned for August 2005 to quantify the guiding performance more accurately so that updates will be available in time for Cycle 15 Phase II proposal preparations.

An important consideration for faint ($m_v \geq 14.0$) guide stars is the possibility that HST may lose lock under special circumstances. The primary concern is that the FGSS used to guide are also providing pointing information to the attitude control system. Loss of lock is expected to occur only if substantial disturbances occur while guiding on faint stars. The gyro pair available in two-gyro mode will affect the probability of loss of lock since the various types of disturbances change the pointing in preferred directions. Simulations of the jitter caused by different disturbances (see below) and the past history of guide star magnitudes in Chapter 7 indicate that loss of lock will occur infrequently, and perhaps only if multiple disturbances are present simultaneously. If loss of lock does occur, science data collection will cease, and it may or may not be possible to resume science observations during the impacted visit. Loss of lock results in the pointing control dropping into T2G mode (if FHST visibility is available) or even into M2G mode (if no FHSTs are available at the time of loss of lock).

5.2 Jitter Overview

5.2.1 Jitter Description

The HST gyroscopes are oriented with respect to each other so that the three functioning gyroscopes can be used to provide three-axis stability for the telescope. Small high-frequency motions of the observatory caused by noise in the gyros and fine guidance sensors, mechanical vibrations, disturbances in the pointing induced by thermal and mechanical effects, gravity gradients across the observatory, and atmospheric drag introduce small changes in the telescope pointing while it is in fine guiding mode obtaining science data. As a result, the HST pointing is constantly changing over very small angular scales that are set by the pointing control law in the altitude control system.

The magnitude of the jitter predicted by simulations below. We provide more information about the sources, frequencies, and two-gyro mode, a comparable jitter magnitude is observed (see Table 1.1). Over 60-second intervals is currently achieved in three-gyro mode. For mode, typical root-mean-square (RMS) pointing jitter of less than ~5 mas expected to be only slightly different in two-gyro mode than in three-gyro mode. Fine-guidance sensors is described by a nearly circular distribution with the fine-guidance sensors is present three-gyro telescope pointing while guiding function of time, the present three-gyro telescope pointing while guiding plotted on the plane of the sky (the V2-V3 observatory plane) as a ellipse defined by the two gyros, the circular jitter distribution becomes an ellipse one axis. With two gyros, the elliptical jitter distribution for a number of gyros from three to two results in a loss of gyro information for points with a typical RMS pointing jitter of <5 mas. Reducing the since there is less precise control in the direction orthogonal to the plane for each possible pair of remaining gyros. The Gyro #6 and #4 are functional but turned off. Table 5.2 lists the angle of the Gyro #6 and #4 are functional but the Gyro axis in each direction is also listed. For reference, Figure 5.2 contains a map of the HST field of view showing the relative positions of the science instruments projected onto the V2-V3 plane.

1. The V1, V2, and V3 coordinate system is sometimes referred to in other HST documents about the V1 axis; pitch occurs about the V2 axis; and yaw occurs about the V3 axis. = -U3 (see Figure 5.2). The plane of the sky lies in the V2-V3 plane. Observatory roll occurs about the V1 axis; pitch occurs about the V2 axis; and yaw occurs about the V3 axis. umenation as the U1, U2, U3 coordinate system, in which V1 = U1, V2 = -U2, and V3 = -U3 (see Figure 5.2).

occurs about the V1 axis; pitch occurs about the V2 axis; and yaw occurs about the V3 axis.

5.2.2 Jitter Orientation

1. The V1, V2, and V3 coordinate system is sometimes referred to in other HST documents about the V1 axis; pitch occurs about the V2 axis; and yaw occurs about the V3 axis. = -U3 (see Figure 5.2). The plane of the sky lies in the V2-V3 plane. Observatory roll occurs about the V1 axis; pitch occurs about the V2 axis; and yaw occurs about the V3 axis. = -U3 (see Figure 5.2). The plane of the sky lies in the V2-V3 plane. Observatory roll occurs about the V1 axis; pitch occurs about the V2 axis; and yaw occurs about the V3 axis.

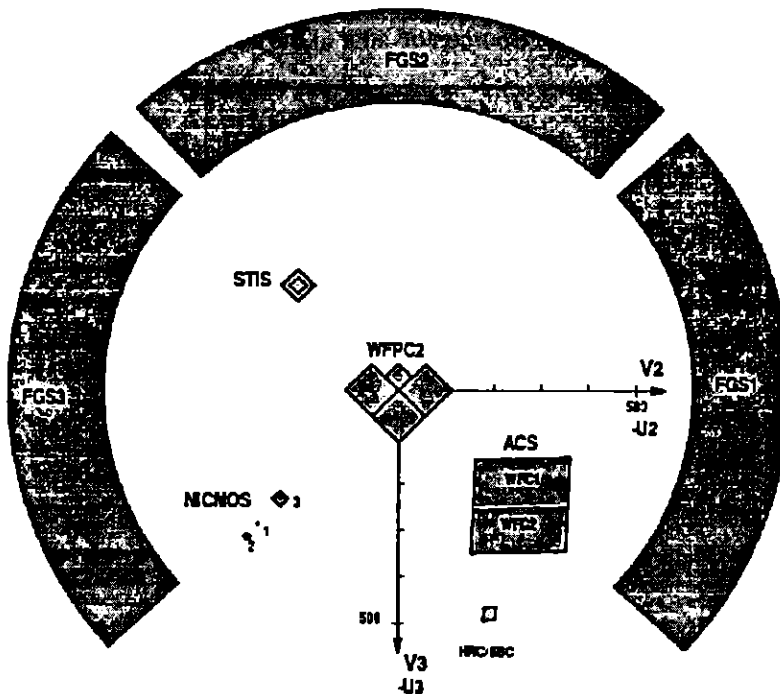
1. The V1, V2, and V3 coordinate system is sometimes referred to in other HST documents about the V1 axis; pitch occurs about the V2 axis; and yaw occurs about the V3 axis. = -U3 (see Figure 5.2). The plane of the sky lies in the V2-V3 plane. Observatory roll occurs about the V1 axis; pitch occurs about the V2 axis; and yaw occurs about the V3 axis.

Table 5.2: Two-Gyro Jitter Ellipse Orientations

Gyro Set	Component of G_x			Angle of G_x Axis on Plane of Sky ¹
	(V1 Direction)	(V2 Direction)	(V3 Direction)	
1 & 2	0.0	1.0	0.0	0.0°
1 & 4	0.5303	-0.7820	-0.3275	-22.7°
1 & 6	-0.5303	-0.7820	0.3275	22.7°
2 & 4	-0.8005	0.3387	-0.4994	55.6°
2 & 6	0.8005	0.3387	0.4994	-55.6°
4 & 6	-0.6678	0.0	-0.7443	90.0°

1. Angle is measured from the V3 axis counterclockwise in the V2-V3 (sky) plane (see Figure 5.2).

Figure 5.2: HST Field of View Following SM3B



5.2.3 Sources of Jitter

There are numerous sources of jitter in the HST pointing, but many of these sources have little impact on the total jitter budget. The dominant sources include thermal gradients across the solar arrays, high gain antenna

The HST pointing is most susceptible to disturbances with frequencies between 0.01 and 0.5 Hz, or periods between 100 and 2 seconds. Higher frequency disturbances damp very quickly. Some sources of jitter (aero and gravity torques, for example) have very low frequencies. The FGs and gyros provide pointing information at a rate of 40 Hz. The pointing control

5.2.4 Jitter Frequencies

Jitter Source	Jitter (mas, 60-sec RMS)	Comment
Solar Array (SA3) Thermal Gradients	8.92	Frequent
V2 Disturbances	4.13	Frequent
High Gain Antenna (HGA) Tracking	3.35	Usually present
Gimbal Articulations	8.02	Intermittent
Reaction Wheel Crossings	2.50	Frequent
Hot altitude	6.00	
FGS PMT + Rate Gyro Noise	3.90	Always present
ACS Filter Wheeles	<2.0	Minimal contribution
SSM Thermal Gradients	1.59	Minimal contribution

Table 5.3: Sources of jitter in the Two-Gyro F2G-FL jitter Budget

Approximate values for the jitter introduced by various sources are listed in Table 5.3. These values are expected to be conservative (generous) estimates of the jitter based upon simulations used to predict the response of HST to disturbances encountered on-orbit. Descriptions of the primary sources of jitter in this table can be found in Section 5.3.

In two-gyro mode, jitter contributions from the combination of rate gyro noise and FGs PMT noise are slightly larger than the rate gyro noise alone in three-gyro mode. The noise introduced into the attitude control law by the Fine Guidance Sensors used to provide pointing control information about the G_x axis is particularly important when faint star measurements are used because of reduced signal-to-noise in the FGs measurements. Information about the jitter caused by rate gyro noise and FGS PMT noise can be found in Chapter 6.

Information about the jitter caused by rate gyro noise and FGS PMT noise is provided to be caused by rotations of the SSM equipment shelf, reaction wheel zero-speed crossings, rate gyro noise, and FGS photomultiplier tube (PMT) noise. Very small contributions (<2 mas) arise from ACS filter wheel motions and SSM thermal gradients.

(HGA) gimbal articulations, occasional disturbances about the V2 axes believed to be caused by rotations of the SSM equipment shelf, reaction

law implemented in the F2G-FL mode has a closed-loop post-filtered bandwidth of ~1 Hz for the entire system, including the G_X axis and gyro plane. Therefore, it is possible to observe and correct for many sources of jitter, even in two-gyro mode.

5.3 Disturbances and Primary Sources of Jitter

There are several types of disturbances that contribute to the jitter expected in two-gyro mode. Below we discuss the most important disturbances listed in Table 5.3.

5.3.1 Solar Array (SA3) Disturbances

Thermal gradients across the third set of HST solar arrays, which were installed during SM3B, lead to several different motions of the solar arrays as they release accumulated stresses. The most important motion is an in-plane bending occurring at a frequency of ~1 Hz. The solar array disturbances occur irregularly; they are not traceable to terminator crossings but are related to the thermal changes caused by the motion of HST around the Earth.

SA3 disturbances last 1-2 seconds and have a variety of amplitudes. Trending of past SA3 events by the HST PCS Group yields the expected frequency of disturbances summarized in Table 5.4. Like the V2 disturbances, the SA3 disturbances are not likely to cause significant data quality degradation unless the event occurs during a short (<10 second) science exposure. Both two-gyro and three-gyro observations are susceptible to these events.

The simulations conducted to date indicate that loss of lock may be an issue in two-gyro mode if SA3 disturbances with amplitudes greater than ~100 mas are encountered. This can be exacerbated if the SA3 disturbance occurs at the same time as disturbances caused by other sources (e.g., high gain antenna gimbal articulations). Loss of lock resulting from SA3 disturbances is most problematic for gyro combination 4-6 (the G_X axis has a significant component in the V3 direction) and least problematic for gyro combination 1-2 (the G_X axis is purely in the V2 direction). The probability of losing lock during an SA3 disturbance in two-gyro mode is higher for fainter guide stars. SA3 disturbances with amplitudes greater than ~300 mas will likely cause loss of lock for any gyro pair with guide star magnitudes $m_V > 14$. Even for bright guide stars (e.g., $m_V < 10$), loss of lock may still occur for gyro pairs 2-4, 2-6, and 4-6 if the SA3 disturbance has an amplitude greater than ~270 mas. Such events are relatively rare (~1 every 20 days). Combining the expected sensitivity of the different gyro pairs to loss of lock, past guide star magnitude distributions, and the SA3

V2 disturbances typically occur in groups of ~5 events, with spacings of a few minutes. The peak-to-peak excursions of the disturbances range from ~25 mas to ~200 mas. The most probable events are those with 50-55 mas amplitudes. Table 5.5 lists the number of expected V2 disturbances per day

its position before the V2 disturbance.

again pointed properly, but the equipment shelf remains rotated relative to their original positions. After this corrective motion, the telescope is once more the bore sight to the proper position necessary to return the stars to commanded motion and feed information into the attitude control loop to correct for the motion. The FGSs, which are guiding on stars, detect this perceived motion of the telescope by commanding the reaction wheels to correct moves, the gyros sense the motion, and the control law reacts to the shelf moves, induce a subsequent telescope pointing change.

The HST gyros and HTSs are mounted to the equipment shelf. When correspond to a movement of the telescope, but the shelf motion does not structure of the shelf over time. The movement of the shelf itself does not be caused by the release of stresses accumulated in the mechanical (SSM) Equipment Shelf about the V2 axis. The motion of the shelf appears to be caused by the rapid motion of the Support Systems Module believed to be caused by the rapid motion of the Support Systems Module (SSM) Equipment Shelf about the V2 axis. The motion of the shelf appears to be caused by the release of stresses accumulated in the mechanical (SSM) Equipment Shelf about the V2 axis. The motion of the shelf appears

V2 disturbances are brief (less than ~ 1 second) impulsive disturbances

5.3.2 V2 Disturbances

Disturbance (mas)	Events/day	>0.01
384.5		
348.1		
310.5		
271.4		
232.4		
194.6		
155.9		
117.6		
80.1	3.32	
43.4	11	

Table 5.4: SAs Disturbance Frequency

disturbance frequencies in Table 5.4, the HST PCS Group predicts <1 loss of lock per day in two-gyro mode.

as a function of amplitude. V2 disturbances are more common for large off-nominal roll angles.

Table 5.5: V2 Disturbance Frequency

Disturbance (mas)	Events/day
55	10.0
60	7.6
65	4.2
70	2.6
75	1.7
80	1.3
85	0.98
90	0.76
95	0.63
100	0.49
105	0.36
110	0.25
115	0.17
120	0.12
200	<0.01

HST is susceptible to V2 disturbances in two-gyro mode as well as three-gyro mode. However, the sensitivity to these disturbances in two-gyro mode will depend strongly on which pair of gyros is operating because the disturbances occur only about the **V2** axis. Gyro combination 1-2 has a G_x axis oriented along the **V2** direction. Therefore, the gyros cannot detect a rotation of the equipment shelf about the V2 axis. As a result, no command would be given to induce telescope motion, and no subsequent command would need to be issued to correct the telescope pointing. Other gyro combinations can sense the shelf rotation; combination 4-6 is the most sensitive since the **V2** axis is completely within the gyro plane. In this case, the behavior of the telescope pointing and the resulting jitter induced by the disturbance would be similar to that encountered in three-gyro mode.

Using the past history of V2 disturbance amplitudes measured on-orbit, the simulations predict that V2 disturbances will not cause loss of guide star lock, even for faint guide stars. These disturbances will not significantly affect data quality of long exposures because the disturbance

HSTSIM is a high-fidelity, non-linear time domain HST pointing performance simulator developed and maintained by the Pointing Control Systems Group at Lockheed Martin Technical Operations (LMTO) Company. It includes realistic models for the HST hardware (FGS, FHTS, gyroscopes, etc.) as well as models of orbital dynamics, the Earth's gravity field, and the Sun's gravitational pull. The software is designed to provide accurate simulations of the HST's trajectory and attitude over long periods of time, taking into account various factors such as the Sun's position, the Earth's rotation, and the effects of the HST's own motion.

5.4 HSTSIM Jitter Simulations

High-rate tracking can also introduce jitter. There are two general types of high-rate tracking - "hardware splines" and "jitter splines". Hardware splines occur at a tracking rate near the hardware limit of 30 degrees per minute. They occur roughly 25 times per week for periods of 5-16 minutes, and they are used only during vehicle slews. They are not currently used and they have tracking rates of <2 degrees per minute, and half have rates of 6-12 degrees per minute. They range from about 10 minutes to 8 hours, which is an average duration of about 1.5 hours. The total fraction of time spent in jitter spline mode is about 50%. The simulations described below include the worst case high-rate tracking jitter expected - about 8 mas RMS averaged over a 60 second time interval.

Jitter (RMS value over a 60 second time interval) is caused primarily by translational bending of the booms along the V1 and V2 axes. It occurs almost constantly since the "ephemeris tracking" is caused primarily by translational bending of the booms along the V1 and V2 axes. It occurs almost constantly since the antennae are often in this tracking mode.

Low-rate tracking during communication contributes about 3-0.5 mas of jitter (RMS value over a 60 second time interval). The jitter induced by this during preparations for communication contributes about 3-0.5 mas of booms along the V1 and V2 axes. It occurs almost constantly since the "ephemeris tracking" is caused primarily by translational bending of the booms along the V1 and V2 axes. It occurs almost constantly since the antennae are often in this tracking mode.

5.3.3 High Gain Antenna Motions

HST has two high gain antenna (HGA) that are used to provide communications with the Tracking and Data Relay Satellite System (TDRSS). The antennae are used to receive commanding instructions and to return engineering and science data. Each steerable HGA sits at the end of a boom extending along the V3 axis and is gimbaled to provide tracking capability as HST orbits the Earth. The gimbal articulations required to position the two HST antennae properly for communications with the TDRSS satellites contribute to the HST jitter budget in two-gyro mode.

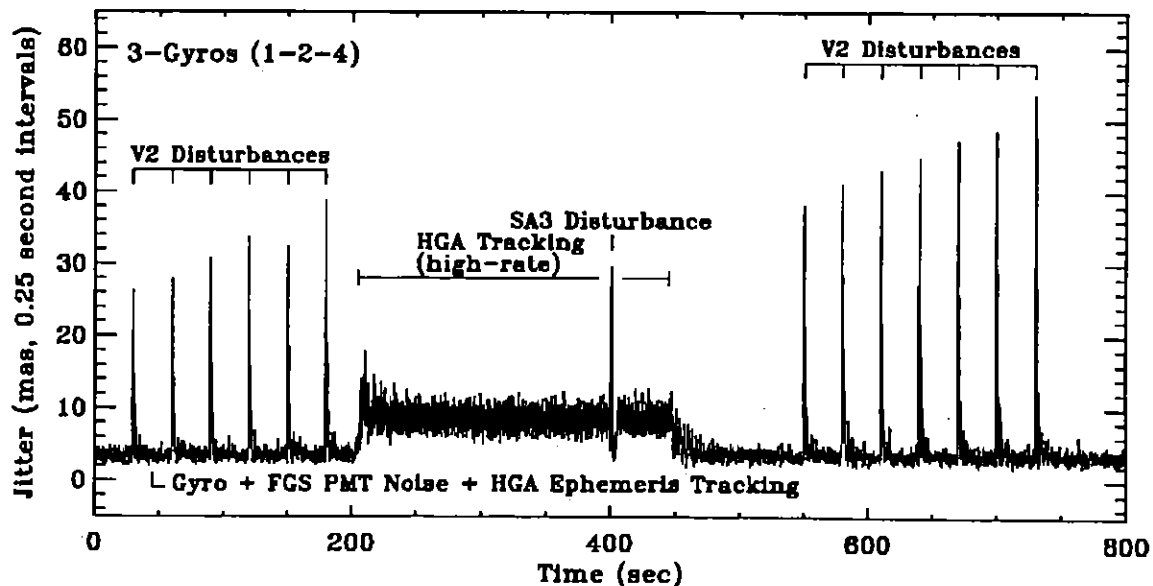
The magnitude of the jitter depends upon the antenna tracking mode. The two-gyro mode provides the best tracking performance, but it requires a significant amount of power and mass. The three-gyro mode provides better tracking performance, but it requires more power and mass. The two-gyro mode is used for most observations, while the three-gyro mode is used for observations in both two-gyro and three-gyro mode.

magnetic field, and sources of attitude disturbances (e.g., high gain antenna moves, V2 and SA3 disturbances, and aerodynamic and gravity gradients). The information in this section is based on the disturbance data analysis and simulations conducted in the summer of 2004 by Brian Clapp and the PCS Group at LMTO.

5.4.1 Integrated Jitter Predictions

HSTSIM models were run for the full range of possible gyro pairs in two-gyro mode. A three-gyro model was also constructed for the currently operating 1-2-4 gyro set. The HSTSIM jitter predictions for three-gyro guiding mode are shown in Figure 5.3, and the predictions for the F2G-FL mode with the 1-4 gyro combination are shown in Figure 5.4. These models incorporate sample disturbances of the type described above, including an SA3 disturbance with an amplitude of 80 mas, thirteen V2 disturbances with amplitudes of 60-120 mas, and HGA tracking disturbances. The timelines shown are not meant to mimic a particular on-orbit combination of disturbance events, but rather are designed to explore the sensitivity of the possible gyro combinations to a variety of different types of disturbances. Clearly, multiple disturbances can be combined to produce larger amounts of jitter.

Figure 5.3: Three-Gyro Jitter Simulation Example with Disturbances



Sample jitter ellipses in the V2-V3 plane are shown in Figure 5.5 for the 1-4 and 2-6 gyro pairs. The data in the upper middle panel corresponds to the jitter time series shown in Figure 5.4 for gyro pair 1-4 with a 13th magnitude guide star. The large excursions caused by V2 disturbances are evident in all six panels. Note the slight increase in jitter as the guide star magnitude increases. The increase in disturbances from 1-4 to 2-6 is also evident. The points in these panels have been binned into 0.25 second jitter averages to make it easier to see these effects. Data from the full 800 stars. The points in these panels have been binned into 0.25 second jitter the increased FGs PMT noise in the simulations with the fainter guide stars. The noise in this jitter increases in this jitter ellipse results from star magnitude increases. The increase in jitter as the guide star is the guide star. The jitter ellipses in the V2-V3 plane are shown in Figure 5.5 for the second simulations are shown.

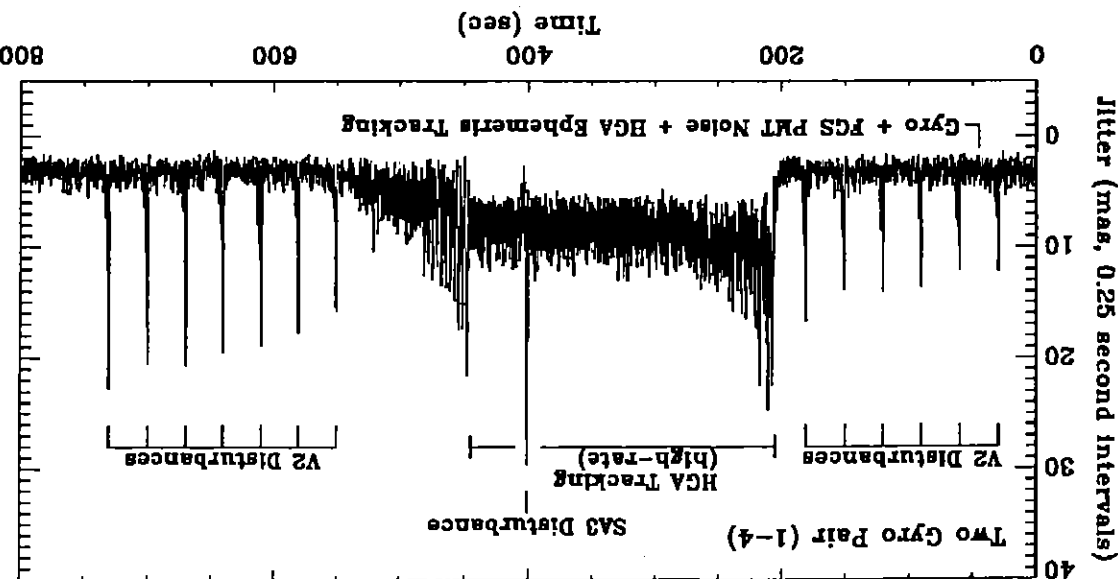


Figure 5.4: F2G-FL Two-Gyro Jitter Simulation Example with Disturbances

Figure 5.5: Jitter Ellipses for Two Possible Pairs of Gyros

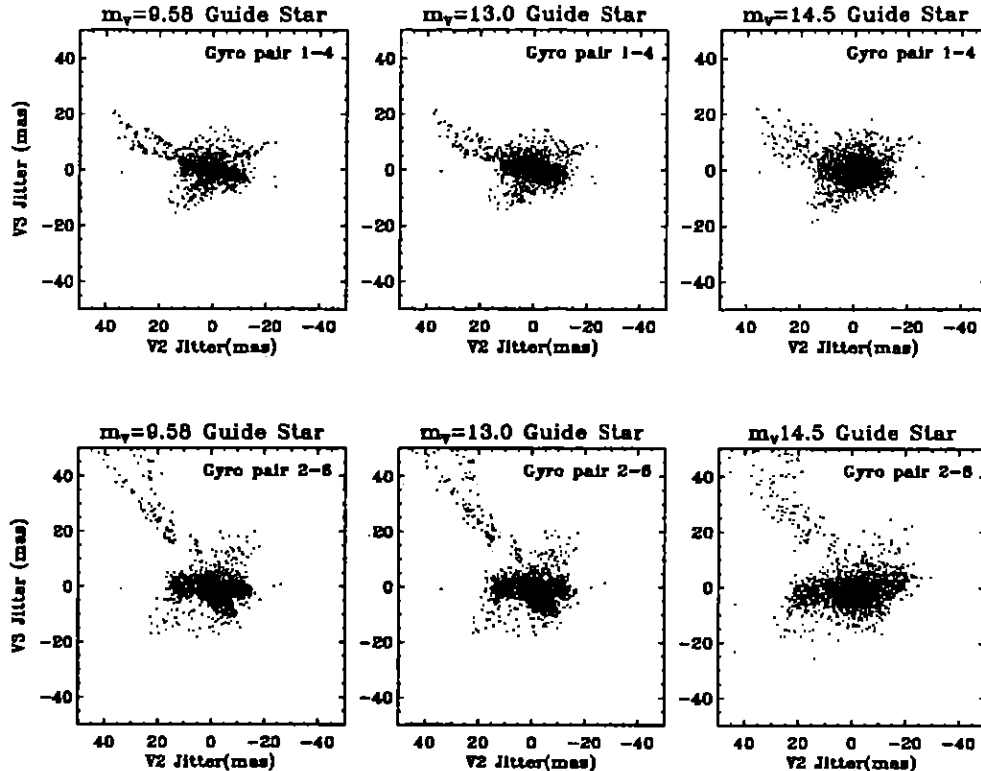


Table 5.6 summarizes the expected jitter in two-gyro mode based upon the HSTSIM predictions. For each possible two-gyro combination and three different FGS guide star magnitudes, the table lists the maximum root-mean-square (RMS) jitter measured in any 60 second interval during the F2G-FL portion of the simulations. The assumptions used in these predictions are the same as those described for the simulation data above. The corresponding values for three-gyro mode are listed at the bottom of the table. Note that these are the maximum values expected; typical jitter values for times between SA3 and V2 disturbances will be considerably less.

1. Angle is measured from the V₃ axis counter-clockwise in the V₂-V₃ (sky) plane (see Figure 5.2).
2. These values are the maximum jitter encountered during any 60 second interval in the F2G-FL portion of the simulation.
3. Loss of lock occurred during SA3 disturbance concurrent with high-rate HGA track.

Gyro Set	Angle of Gyro Axis on Plane (mas, 60-second RMS) ²	$m_V = 9.58$	$m_V = 13.0$	$m_V = 14.5$
Two-Gyro F2G-FL Results				
1-2	0.0	9.55	9.76	10.40
1-4	-22.7	10.65	10.86	11.65
1-6	22.7	11.72	11.91	13.06
2-4	55.6	12.20	12.30	15.97
2-6	-55.6	12.39	12.47	17.41
4-6	90.0	12.26	12.49	18.93
Three-Gyro Results				
1-2-4	N/A	9.73	9.73	9.75

Table 5.6: Two-Gyro and Three-Gyro Jitter Predictions (including Disturbances)

CHAPTER 6:

Quiescent F2G-FL Jitter Predictions

In this chapter . . .

6.1 HSTSIM Quiescent Jitter Predictions / 59

6.1 HSTSIM Quiescent Jitter Predictions

Estimates of the magnitude of the jitter in F2G-FL mode caused by rate gyro noise and FGS photomultiplier tube (PMT) noise are listed in Table 6.1 for various combinations of guide star magnitudes ($m_v = 9.58, 13.0$, and 14.5) and possible gyro pairs. The jitter values listed are the maximum values expected for a 60 second exposure; they are only slightly larger than those predicted for the gyro noise in three-gyro mode. These “quiescent” simulations include only the jitter contributions from these two sources and do not include more prominent contributions from the on-orbit disturbances that contribute to the overall jitter budget discussed in Chapter 5.

Sample two-gyro jitter ellipses in the V2-V3 plane caused by rate gyro noise and FGS PMT noise are shown in Figure 6.1 for the 1-4 and 2-6 gyro pairs. No disturbances are included in these simulations; see Chapter 5 for a similar figure that includes disturbances. In the quiescent simulations, the shape of the jitter in the V2-V3 plane depends strongly on the magnitude of the guide star used by the FGS to measure motions about the G_X axis. For bright guide stars, the FGS measures motions about the G_X axis very precisely, and the jitter is elongated in a direction corresponding to measurement of motions by the gyros (i.e., most of the jitter is contributed by gyro noise rather than FGS PMT noise – see the left panels in the figure). For faint guide stars, the jitter shape becomes more circular, with an increase in the magnitude of the jitter in the direction corresponding to

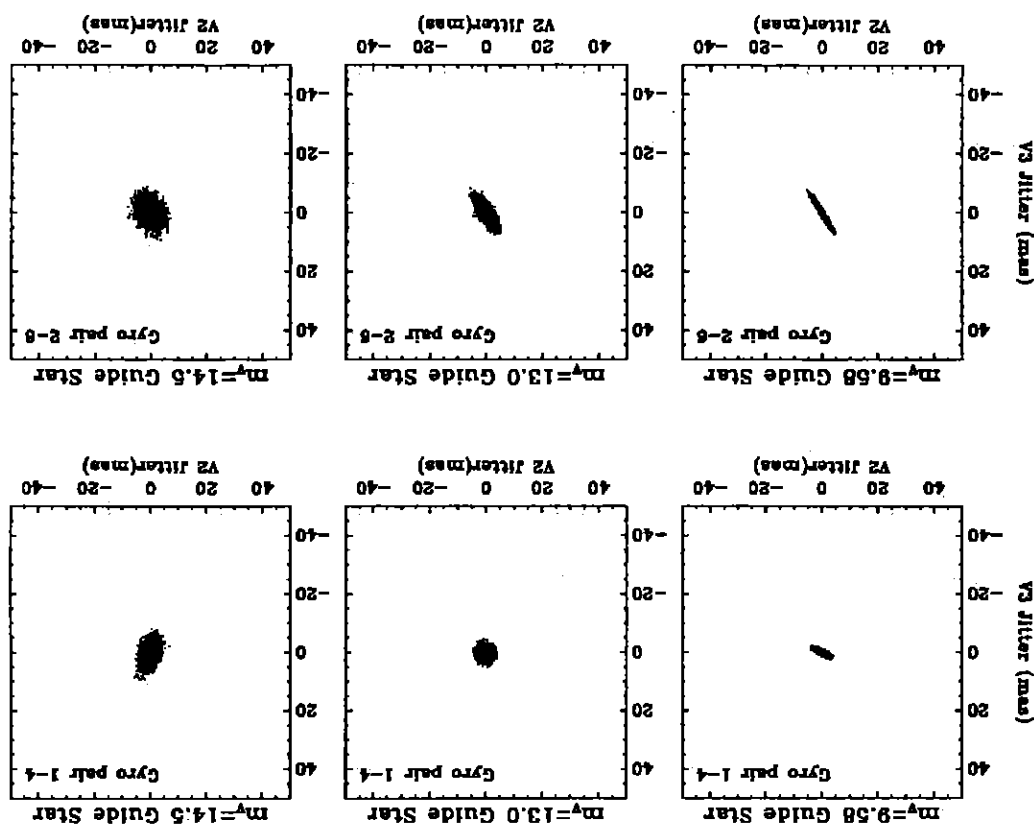


Figure 6.1: Jitter Ellipses Resulting from Rate Gyro Noise and FGS PMT

1. Angle is measured from the V3 axis counter-clockwise in the V2-V3 (sky) plane (see Figure 5.2).
2. These values reflect only the jitter caused by rate gyro noise and FGS PMT noise.

Gyro Pelt	Angle of Gyro Axes on Plane of Sky	Maximum F2G-FL Bore sight jitter (mas, 60-second RMS) ²	$m_V = 9.58$	$m_V = 13.0$	$m_V = 14.5$
4-6	90.0	1.48	2.03	3.38	
2-6	-55.6	2.62	2.90	3.93	
2-4	55.6	2.70	2.88	3.89	
1-6	22.7	1.29	1.85	3.42	
1-4	-22.7	1.28	1.78	3.42	
1-2	0.0	1.17	1.63	3.20	

Table 6.1: Quiescent Two-Gyro jitter Predictions (No Disturbances)

the measurement of motions about the G_X axis (i.e., PMT noise becomes more prominent – see right panels in the figure).

CHAPTER 7:

Guide Star Magnitudes

In this chapter . . .

7.1 Guide Star Magnitude Tables / 61

7.1 Guide Star Magnitude Tables

The following tables contain information about the brightness distributions of guide stars in the three Fine Guidance Sensors from January 2000 through August 2004. Both dominant and secondary guide stars are included. A small number of these guide stars resulted in failed acquisitions.

The magnitude distributions are based upon the predicted (catalog) magnitudes of the guide stars. The typical uncertainty in the magnitudes is 0.3-0.5 mag. Although it is possible to use guide stars fainter than $m_V = 14$, few such instances occur since brighter guide stars can usually be found.

mV	Y2000	Y2001	Y2002	Y2003	Y2004	2004)
	Total	1652	1751	1645	2004	1600
Percentage of Guide Stars Brighter than Listed Magnitude (8652 total, 5833 unique)						
9.5	1.2	2.0	2.5	1.6	1.9	
10.0	3.5	6.8	8.6	6.0	5.9	
10.5	6.3	13.3	15.0	10.8	10.5	
11.0	11.0	21.4	22.4	17.8	17.1	
11.5	17.7	34.2	36.5	25.5	27.6	
12.0	26.4	47.7	52.0	43.1	39.9	
12.5	39.2	61.1	64.7	57.1	54.6	
13.0	55.9	74.5	76.5	75.0	68.7	
13.5	75.8	88.1	88.0	87.7	84.1	
14.0	99.8	99.7	99.5	99.3	99.9	
14.5	100.0	100.0	100.0	100.0	100.0	
Percentage of Guide Stars Brighter than Listed Magnitude (8876 total, 6003 unique)						
mV	Y2000	Y2001	Y2002	Y2003	Y2004	2004)
Total	1135	1983	1886	2060	1812	

Table 7.1: HST FGS1 Guide Star Brightness Distribution (January 2000 - August 2004)

mV	Y2000	Y2001	Y2002	Y2003	Y2004	2004)
	Total	1135	1983	1886	2060	1812
Percentage of Guide Stars Brighter than Listed Magnitude (8876 total, 6003 unique)						
9.5	1.1	3.4	2.4	2.0	1.8	
10.0	4.2	8.6	7.4	5.9	5.2	
10.5	8.2	15.5	13.8	11.6	10.5	
11.0	12.7	25.0	23.5	19.1	17.3	
11.5	18.4	34.5	35.4	28.9	24.8	
12.0	27.5	49.4	49.8	42.9	38.0	
12.5	41.9	63.3	64.2	54.1	52.4	
13.0	58.3	77.2	76.9	71.5	68.7	
13.5	76.7	89.9	87.4	84.4	84.5	
14.0	99.6	100.0	99.9	99.7	99.9	
14.5	100.0	100.0	100.0	100.0	100.0	
Percentage of Guide Stars Brighter than Listed Magnitude (8876 total, 6003 unique)						
mV	Y2000	Y2001	Y2002	Y2003	Y2004	2004)
Total	1135	1983	1886	2060	1812	

Table 7.2: HST FGS2 Guide Star Brightness Distribution (January 2000 - August 2004)

Table 7.3: HST FGS3 Guide Star Brightness Distribution (January 2000 - August 2004)

m_V	Percentage of Guide Stars Brighter than Listed Magnitude (8387 total, 5744 unique)				
	Y2000	Y2001	Y2002	Y2003	Y2004
9.5	1.2	2.3	2.8	2.5	5.0
10.0	3.3	7.2	7.5	6.1	6.8
10.5	7.2	12.8	13.7	11.4	12.6
11.0	11.7	20.8	23.6	24.8	16.6
11.5	18.2	31.7	33.5	34.4	25.4
12.0	27.9	46.2	48.3	46.6	35.9
12.5	41.7	59.9	62.1	61.5	47.3
13.0	58.7	75.8	76.5	75.3	64.5
13.5	76.1	89.4	87.2	88.6	80.6
14.0	100.0	99.9	99.6	99.7	99.9
14.5	100.0	100.0	100.0	100.0	100.0
Total	2050	2013	1769	1792	763

Glossary

The following terms and acronyms are used in this Handbook.

- ACS:** Advanced Camera for Surveys
- ACS / HRC:** ACS High-Resolution Channel
- ACS / SBC:** ACS Solar-Blind Channel
- ACS / WFC:** ACS Wide-Field Channel
- APT:** Astronomer's Proposal Tools
- CP:** Call for Proposals
- CCD:** Charge-coupled device
- CVZ:** Continuous viewing zone
- ETC:** Exposure time calculator.
- F2G:** Fine guidance sensor / two-gyro (mode)
- FAQ:** Frequently asked questions
- FGS:** Fine Guidance Sensor
- FGS1r:** Fine Guidance Sensor replacement for FGS1 (in SM2)
- FRB:** Failure Review Board
- FHST:** Fixed-head star tracker
- GO:** Guest Observer
- HDF:** Hubble Deep Field
- HGA:** High gain antenna
- Help Desk:** Facility for getting help on HST related topics via email.
help@stsci.edu.
- HST:** Hubble Space Telescope
- HUDF:** Hubble Ultra-Deep Field
- HV:** High voltage
- NICMOS:** Near-Infrared Camera and Multi-Object Spectrograph
- mas:** milli-arcseconds
- M2G:** MSS / two-gyro (mode)
- MSS:** Magnetic Sensing System

<i>OBA</i>	Onboard attitude determination
<i>PC</i>	Pointing control system
<i>Phase I proposal</i>	A proposal for observing time on HST
<i>Phase II program</i>	An approved HST program; includes precise detail of how program is to be executed
<i>PI</i>	Principal investigator
<i>PMT</i>	Photomultiplier tube
<i>POS</i>	Positional (mode of FGS operation)
<i>PSF</i>	Point spread function
<i>RA</i>	Right Ascension (also denoted by "a")
<i>RMS</i>	Root-mean-square
<i>RSU</i>	Rate sensing unit
<i>SAA</i>	South Atlantic anomaly
<i>SA3</i>	Solar arrays (third set installed during SM3B)
<i>SAZ</i>	Solar avoidance zone
<i>SM</i>	Service Mission (as in SM1, SM2, SM3A, SM3B)
<i>SNOV</i>	Service Mission Observatory Verification
<i>SNAP</i>	SNAPSHOT (type of HST observation)
<i>SNR</i>	Signal-to-noise ratio
<i>SSM</i>	Support Systems Module
<i>STIS</i>	Space Telescope Imaging Spectrograph
<i>STS</i>	Space Transport System (Space Shuttle)
<i>STScI</i>	Space Telescope Science Institute
<i>T2G</i>	FHST / two-gyro (mode)
<i>TAC</i>	Time Allocation Committee
<i>TDRSS</i>	Tracking and Data Relay Satellite System
<i>TGS</i>	Two-Gyro Science
<i>TOO</i>	Target of opportunity
<i>TRANS</i>	TRANSFer (mode of FGS operation)
<i>URL</i>	Uniform resource locator
<i>WFPC2</i>	Wide Field Planetary Camera-2
<i>WWW</i>	World Wide Web
<i>ZGSP</i>	Zero-gyro sunpoint (safe mode)

Index

A

- All-sky availability/schedulability
 - Fixed targets 8, 9, 10
 - Movie 9
- Assessing scheduling and visibility 11

C

- Continuous Viewing Zones (CVZs) 10, 30

D

- DayOrientPlot 15
- DetailedPlot 21

F

- F2G 41, 42, 50
- Fine Guidance Sensors
 - Gx axis control 38, 50, 57

G

- Guide star acquisitions 45
 - Acquisition times 46
 - Loss of lock 47
- Guide star magnitudes 46, 61, 62, 63
- Guiding performance in two-gyro mode 47
- Gx axis 38, 39, 40, 41, 43, 48, 49, 50, 51, 53, 58, 59, 60
- Gyro plane 38, 39, 40, 51, 53
- Gyroscope 33, 34, 35, 36
- Gyroscope replacements 36

J

- Jitter
 - Frequencies 50
 - HSTSIM jitter simulations 54, 55, 57, 59
 - Orientation of jitter ellipse 48, 49
 - Sources 49, 50, 51

M

- M2G 39, 42
- Magnetic Sensing System (MSS) 39, 42, 43
- Moving targets 31

O

- OrientMonthPlot 17

P

- Pointing constraints 43
- Pointing control modes
 - F2G 41, 42, 50
 - M2G 39, 42
 - T2G 40, 41, 42
- Pointing Disturbances
 - HGA motions 50
- Pointing disturbances
 - HGA motions 50, 54, 55
 - SA3 disturbances 50, 51, 52, 55, 57
 - V2 disturbances 50, 51, 53, 55, 56

T

- T2G 40, 41, 42
- Tools for observers
 - Astronomer's Proposal Tool (APT) 30

- Detailed Visibility tool 21
- Exposure Time Calculators (ETCs) 30
- Target Visibility and Orientation tool 14
- Two-gyro coordinate convention 38
- Two-gyro scheduling examples 22, 25, 28
- Two-Gyro Science web page 14, 21, 23, 24, 30,